Unfavorable Geology and Mitigation Measures for Water Inrush Hazard during Subsea Tunnel Construction: A Global Review

Fangyuan Niu [1,2], Yuancheng Cai [3], Hongjian Liao [1,*], Jigang Li [3], Kunjie Tang [3], Qiang Wang [3], Zhichao Wang [3], Dedi Liu [3], Tong Liu [4], Chi Liu [3,5] and Tao Yang [6]

1   School of Human Settlements and Civil Engineering, Xi'an Jiaotong University, Xi'an 710049, China; niufy@chd.edu.cn
2   China Construction Silk Road Construction Investment Co., Ltd., Xi'an 710075, China
3   School of Highway, Chang'an University, Xi'an 710064, China; caiyuancheng@chd.edu.cn (Y.C.); jigangchd@163.com (J.L.); Tangkunjie@chd.edu.cn (K.T.); wangqiang123@chd.edu.cn (Q.W.); wangzc@chd.edu.cn (Z.W.); L17633883170@163.com (D.L.); liuwei_7523@163.com (C.L.)
4   School of Science, Xi'an University of Architecture and Technology, Xi'an 710055, China; liutong@xauat.edu.cn
5   Zhengzhou Airport Economy Zone, Urban Development LLC, Zhengzhou 451162, China
6   Sichuan Dujin Mountain Rail Transit Co., Ltd., Aba Tibetan and Qiang Autonomous Prefecture, Chengdu 623006, China; yangtao9508@foxmail.com
*   Correspondence: hjliao@mail.xjtu.edu.cn

Abstract: Water inrush hazard seriously threatens construction safety of subsea tunnels in unfavorable geological areas. In recent years, a large number of subsea tunnels have been built worldwide, some of which have experienced many water inrush disasters, especially in Japan and Norway. In this paper, a systematic methodology is proposed to rigorously review the current literature about water inrush in subsea tunnels. Emphasis is placed on recorded causes and evolution processes of water inrush, as well as relevant mitigation measures. In particular, the geological conditions that generate such water inrush hazards are initially discussed by counting cases of tunnel water inrush in the past decades (43 cases of water inrush hazards in tunnels (including mountain tunnels)). The process of formation of failure modes of water inrush, and the corresponding research methods (including theoretical, numerical and experimental) are reviewed, and can be used to pave the ways for hazard prevention and future research. This is followed by a summary of the prevention methods and mitigation measures used in practice, and a short discussion of the achievements and limitations of each method. Then combined with the evolution characteristics of the failure area, the water inrush process of different modes is divided into three stages, with a proposed a grouting scheme for each stage. Finally, concluding remarks, current research gaps and future research directions on subsea tunnel water inrush are provided and discussed.

1. Introduction

In the past 15 years, submarine tunnels have developed extremely rapidly worldwide, especially in China. By the end of 2020, as many as 154 submarine tunnels were under construction, with the largest number of tunnels crossing the waters of the Huangpu, Pearl, and Yangtze rivers [1]. Additionally, a large number of subway tunnels, diversion tunnels and utility tunnels are currently under construction. Tunnels will be constructed at an annual increasing rate of 7% worldwide for the next 5 to 10 years (equating to 5200 km of tunnels being built every year) [2].

With the rapid development of mechanization and automation in tunnel construction, the size, section and span of tunnels are increasing. The possibility of facing geological hazards, mainly water and mud inrush, is also increasing. In fact, since the 1950s, more than

200 water and mud intrusions (including in subsea tunnels) have been reported worldwide, resulting in huge casualties, economic losses, and environmental damage [3–7], as shown in Figure 1. For example, on 10 June 2018, about 57,000 m^3 of water continuously entered the palm face of the Chaoyang Tunnel excavation within 40 min. An excavation bench (1800 m away from the structural opening in the tunnel) and a lining trolley (716 m away from the structural opening in the tunnel) were flushed out of the hole due to the huge water pressure [8]. On 15 July 2021, the Shijingshan Tunnel encountered a water-rich weathering trough while crossing the F69 fault. Due to improper construction methods and a lagging support system, the arch of the east tunnel collapsed and was flooded. A hydraulic connection was formed between the Jida Reservoir and the tunnel, followed by a large amount of mud and sediment gushing into the west tunnel, resulting in the drowning death of the operator [9]. The Shangjiawan Tunnel [10] uncovered a large infill cavern by the arch wall on 4 June 2013, causing water and mud surges in the lower right side of the palm face. The instantaneous water and mud inrush amounted to 7700 m^3. A total of three large water inrush disasters occurred during the construction of the Denghuozhai Tunnel, the largest of which occurred on 13 May 2012. About 100 m of the tunnel was completely filled with surge sediment, and the huge force pushed the support frame about 100 m towards the entrance [11].
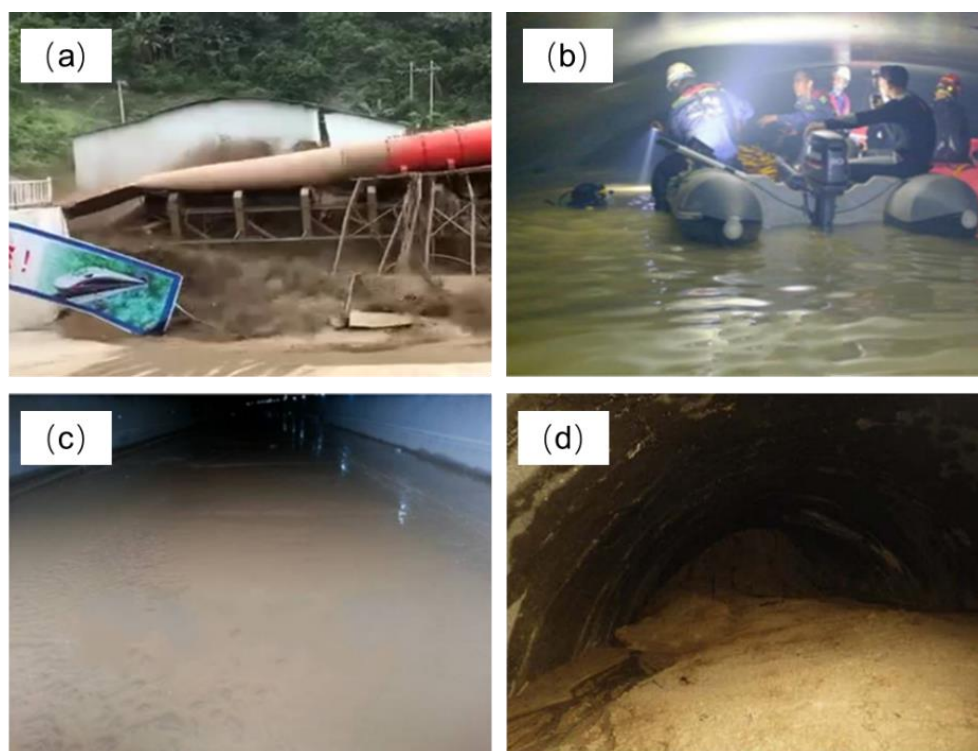

Figure 1. Water inrush in tunnels: (**a**) Chaoyang Tunnel [8]; (**b**) Shijingshan Tunnel [9]; (**c**) Shangjiawan Tunnel [10]; (**d**) Denghuozhai Tunnel [11].

Compared to mountain tunnels, subsea tunnels, as a large high-risk projects, usually have a "V"-shaped longitudinal section [12–15] and unlimited water recharge, so there is a higher possibility of water surges during construction, especially when crossing unfavorable geology. For example, the Seikan Tunnel in Japan had four large scale water inrush disasters during the construction process, which caused major casualties. During the construction of the Oslo-fjord Tunnel in Norway, a massive zone of loose sediment was encountered, and the section was only passed without danger by freezing the ground. The Storebaelt Channel Tunnel in Denmark also experienced several water inrush hazards when crossing the marl aquifer. Water inrush disasters also occurred when the Xiang'an

Tunnel in China crossed a completely weathered trough and an F4 strongly weathered capsule in the sea area, which caused great difficulties in construction [16–18].

After the construction of subsea tunnels, the surrounding rock is damaged and destroyed under the coupling action of seepage field and stress field [19]. When groundwater breaks through the water blocking structure and suddenly enters the tunnel, this is called a water inrush hazard, which is rapid and fierce, and the amount of water inrush is large. This hazard may occur when the tunnel construction is close to or through caves, faults or strong weathering zones, and other geological features. These geological features are often referred to as "unfavorable geology" and are the main cause of water and mud inrush surges [20].

Earth stress, earthquake, blasting and other external forces may also make weak rock collapse and deteriorate, producing geological fractures, forming water inrush channels, and eventually causing the influx of muddy water [21,22]. In the past 30 years, to explore the evolution process and mechanisms of tunnel water inrush, model tests, numerical simulations, field tests and other research methods have been widely used [23–25]. However, they have been basically focused on single field research. In practical projects, tunnel water inrush hazards often occur due to multiple factors. At present, there are few studies on this point, and further exploration is needed to make up the gap.

The proposed mitigation measures for water and mud inrush hazards have important engineering significance for subsea tunnels [26]. At present, there is much research on prevention and control measures, and some useful methods and technologies have been developed, such as advanced geological prediction, field monitoring technology and composite grouting measures [27–29].

This paper summarizes the research status of water and mud inrush hazards in subsea tunnel engineering. It starts with a discussion of the causes of water and mud inrush, by reviewing hazard cases since the 1950s. This is followed by a review on the various evolution processes and corresponding research methods for this hazard. Subsequently, the paper provides a summary of relevant hazard prevention methods employed by academics and practitioners. The technical difficulties of tunnel construction, waterproofing and drainage, and the evolution process of the three water inrush modes are compared and discussed, and reinforcement measures are proposed for different modes. At same time, this study also classifies the previous research landscape of submarine tunnels and considers emerging lines of research. Finally, current gaps in the field are identified in an attempt to direct further research.

2. Materials and Methods

2.1. Literature Retrieval

Relevant research articles were searched using the subject queries illustrated in Figure 2. The subjects were divided into two parts. The first part was to find the articles related to tunnel water inrush, and the second part was to limit the search results to articles studying subsea tunnel water inrush. Seven online databases were employed to conduct a full-text search using the adopted query. The databases contain: "CNKI" [30], "Science Direct" [31], "Springer Link" [32], "Engineering Index" [33], "Web of Science" [34], "Taylor & Francis" [35], "ASCE Library" [36]. In addition, a search of the titles and abstracts was carried out. Advanced search options in the databases were utilized to include journal and conference papers only, while other types were eliminated.

The resulted articles were screened in two rounds. In the first round, all irrelevant articles were excluded by checking the title and abstracts. In the second round, the full text of the article was extensively reviewed to ensure that the included articles were consistent with the adopted criteria. The adopted inclusion criteria are as follows: (1) published in a journal or conference proceedings; (2) include experimental, field or numerical investigation; (3) focus of the article was to explore the evolution process and prevention measures of water inrush hazard. In the second round, the full text of the article was extensively

reviewed to ensure that the included articles were consistent with the adopted criteria. The last update of retrieval time was in April 2022.
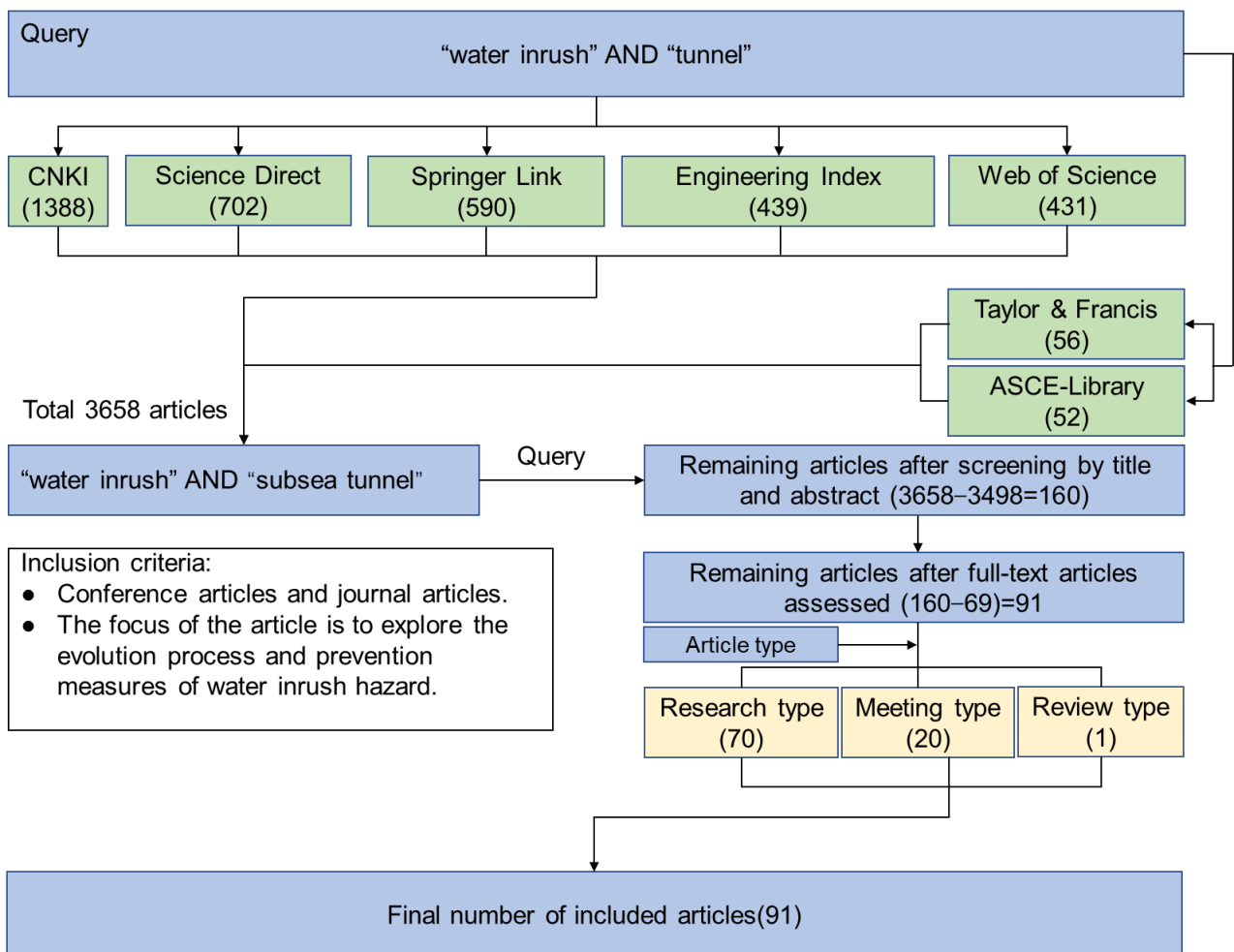
Figure 2. System review process.

The initial query search found 3658 articles published between 2000 and 2022. In the first round of screening for scanning titles and abstracts, 3498 articles were excluded. In the second round of full-text reading, another 69 articles were excluded, leaving 91 articles to be finalized.

2.2. Search Results Analysis

The article screening process in Figure 2 was used to generate the taxonomy shown in Figure 3. This taxonomy provides an extensive list of research related to water inrush in subsea tunnels in recent years. As shown in Figure 3, a wide range of research attempts have been made by scholars to explore the mechanisms of tunnel water inrush evolution, and preventive and curative measures, through the use of field monitoring, model tests, numerical simulations and other methods.

The first analysis showed that research articles accounted for the majority, about 76.9%, followed by conference articles and review articles. To date, research on subsea tunnels has been very extensive, but there is a lack of summaries of results and perspectives on future research directions. Secondly, by reading the literature, it was found that more than 39.6% of the articles were concerned with the prediction and risk assessment of water inrush in tunnels, while the remaining articles were mostly focused on the simulation of seepage in fractured rock and new technologies for grouting.
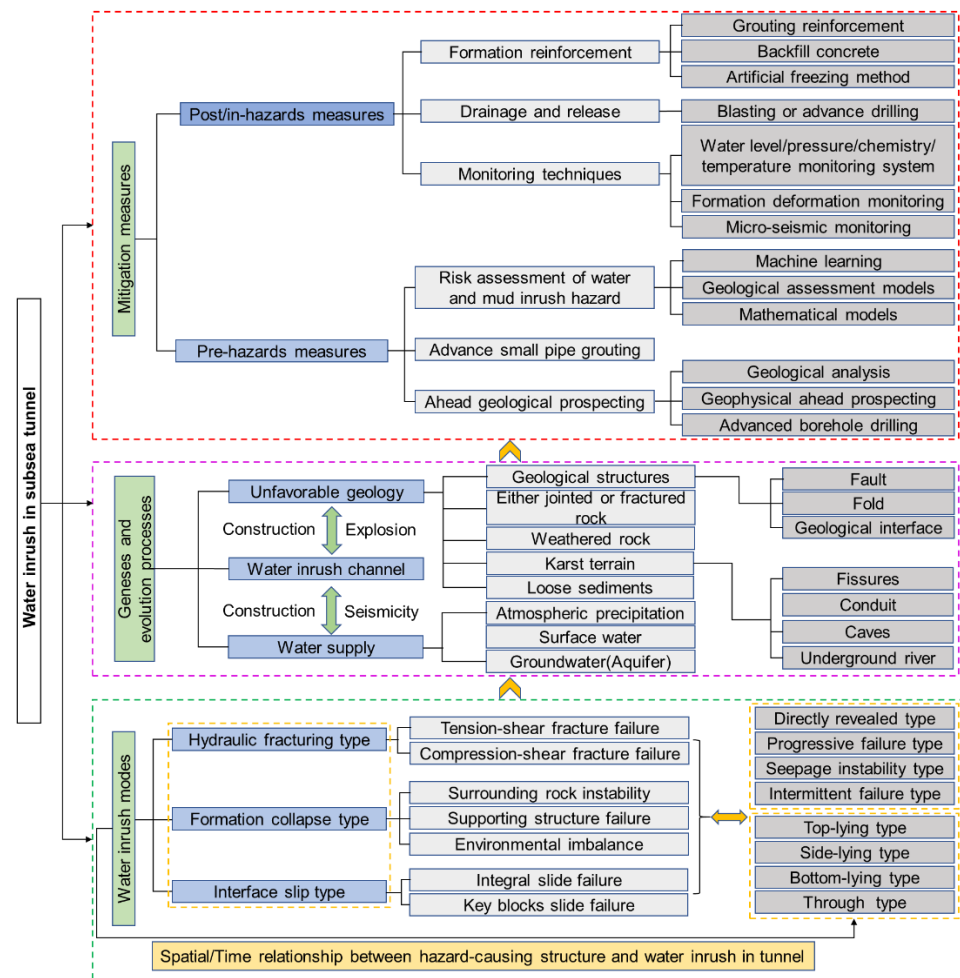
Figure 3. Taxonomy of research literature on water inrush in subsea tunnel.

3. Causes of Water Inrush in Subsea Tunnels

Water inrush in a tunnel is the result of the combined effect of regional geological conditions, hydrological conditions and tunnel construction disturbances. The occurrence of water inrush requires various conditions, such as a steady stream of water sources, water channels, and unfavorable geology, as shown in Figure 4.

Figure 4. Water inrush conditions.

3.1. Unfavorable Geological

(1) Fault Tunnel geological exploration is difficult, and the investment is large. When water inrush occurs, a fault with cracks is the preferred n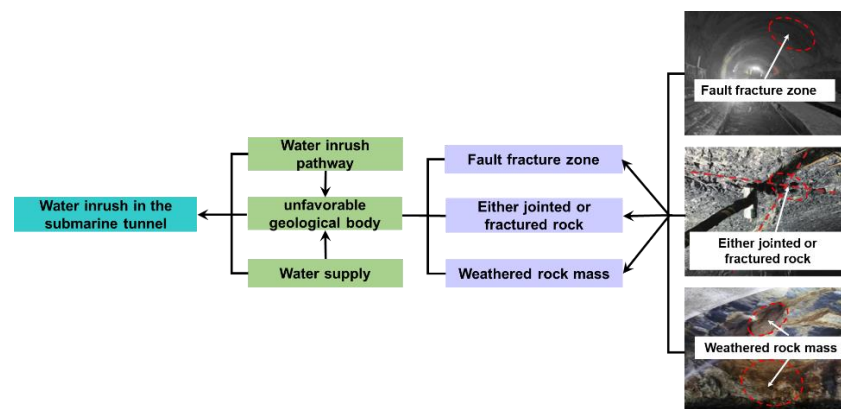atural plane for water inrush. Nilsen [37,38] pointed out that a fault was the most unstable factor by analyzing water inrush problems in the construction of the Ellingsøy and Vardø Tunnels in Norway. After water inrush of the Old Dana Tunnel in Japan, an investigation of the geological conditions of the accident revealed that the presence of a fault fracture zone led to its destabilization and damage under high water pressure, resulted in serious consequences. Relevant studies show [39,40] that the strike, dip angle, width of fault fracture zone, the degree of rock fracture, the activity of groundwater and the spatial relationship with the tunnel can have important impacts on the stability of the tunnel.

(2) Jointed or fractured rock Most water inrush is accompanied by surrounding rock conditions with jointed fissures. Under the influence of engineering disturbance, surrounding rock stress is concentrated, and the existing jointed fissures begin to expand. In this process, the mechanical parameters of rock damage are reduced due to deterioration, and the adjacent joint fissures expand and connect with each other. For example, stress concentration made the existing cracks in the Slemmestad and Vollsfjord Tunnels in Norway [41,42] develop and connect with seawater. and high pressure caused the cracks to penetrate and form water-conducting passages [43–47]. During the construction of the Qingdao Jiaozhou Bay Tunnel in China [48], the back of the initial support fell off, and water was hydraulically split along existing fissures to form a water channel.

(3) Weathered rock Typical weathered rock is easily softened when it meets water [49]. When a tunnel passes through this kind of rock mass, due to its poor stability, formation collapse occurs and induces water inrush. The most representative weathered rock is an undersea weathered trough, which is prone to water inrush due to direct communication between fissures and seawater (Figure 5). For example, in October 2006, a large-scale water inrush occurred when the Xiang'an Tunnel [19] crossed the F1 weathered trough, and disintegration of surrounding rock in water reached 80%.
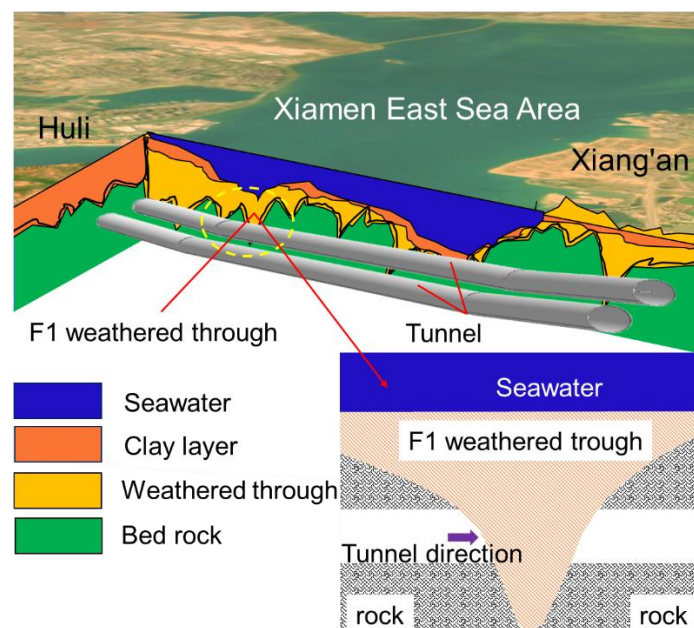

Figure 5. Relative position of Xiang'an Subsea tunnel and F1 weathering trough [19].

3.2. Water Supply

The water supply of a subsea tunnel mainly comes from atmospheric precipitation, surface water, and groundwater [50–53]. Atmospheric precipitation infiltration is the

main source of replenishment of groundwater. Groundwater can enter the tunnel during excavation and become the main source of replenishment (Figure 6). Surface water comes from surface water bodies near tunnels in land areas, such as depressions between hills, plain rivers, and fishponds, which are less likely to become the source of water inrush. Unfavorable geological fissures contain abundant water, which are infiltrated by the surface water and closely connected with seawater. The fissures complement each other, are easily disturbed by excavation, and become the main source of water inrush. Therefore, only by distinguishing the main and secondary water sources can we more effectively prevent a tunnel water inrush hazard.
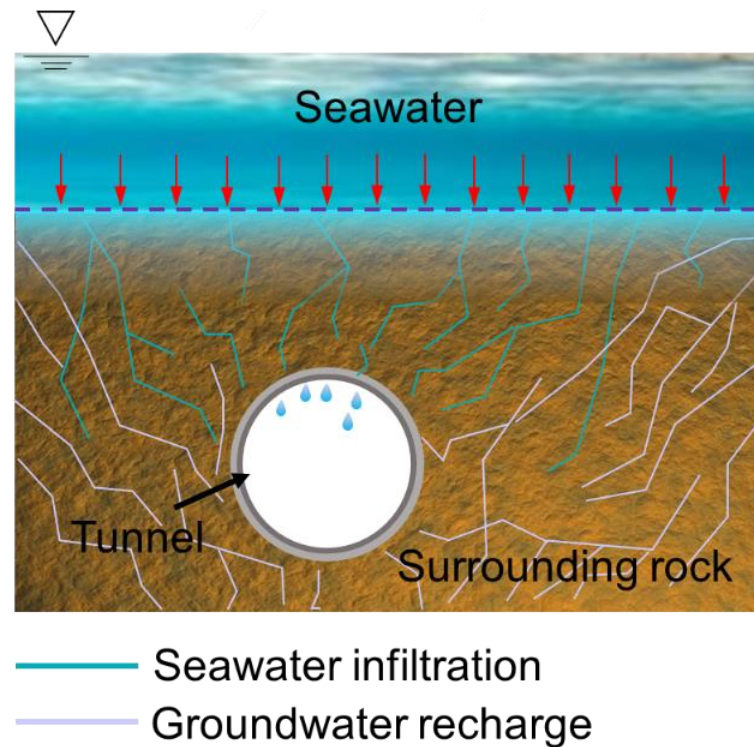

Figure 6. Tunnel water supply.

3.3. Water Inrush Channel

The formation of a water inrush channel is affected by both geological and hydrological conditions [54], as shown in Figure 7. Specifically, in areas with fractured zones in unfavorable geological, water usually infiltrates along contact interfaces such as jointed or fractured and faults [55,56]. Under the action of hydraulic pressure, fractured fault zones, jointed fissures, and caves are natural water storage and water-conducting structures. On the one hand, in the case of connection with water sources, fault, jointed and fractured zones, and caves are natural water storage and conductive structures. Under the action of high pressure, the flowing groundwater fills fractures and the small particulate matter in the fracture zone, forming a water inrush channel [57,58]. On the other hand, under the combined effect of excavation disturbance and groundwater, tunnels crossing weathered grooves and ground interfaces are often prone to cause deformation of surrounding rock, generating cracks to form water inrush channels [59–61]. Therefore, an unfavorable geological body is not only a space for groundwater transport and storage, but also, under the influence of tunnel excavation, is often accompanied by the formation of water inrush channels.
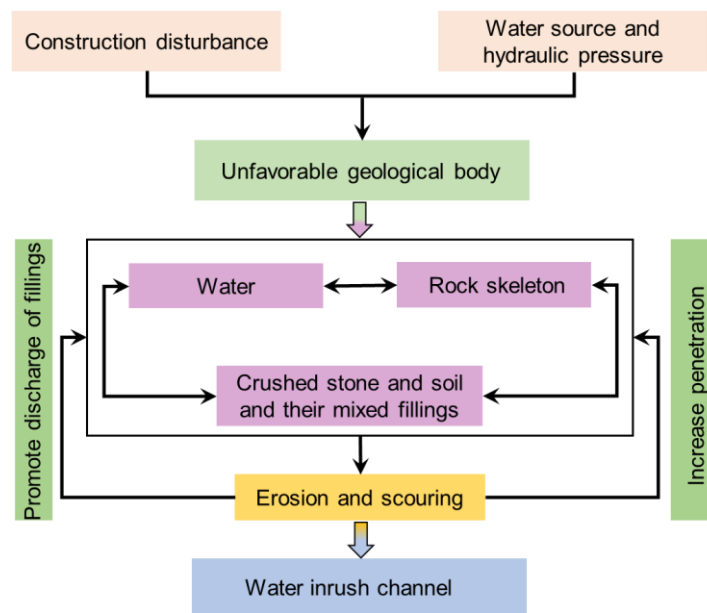
Figure 7. Formation process of a water inrush channel.

4. Water Inrush Modes

4.1. Statistical Investigation of Tunnel Water Inrush Accidents

To study the hydrogeological conditions and mechanical characteristics of water inrush hazards in tunnels, a database was established. Through it, common and individual problems in the process of water inrush and post-disaster reinforcement measures were explored. Because the data in some cases were not detailed enough, this paper was not limited to the statistics of subsea tunnels. Specific statistical analysis is shown in Table 1.

Table 1. Statistics of tunnel water hazard cases.

Tunnel Name	Unfavorable Geology	Water Supply	Causes of Water Inrush	Water Inrush Scale	Reinforcement Measure
Yuanliangshan Tunnel (China)	Jointed and fractured rock	K-W	Rock mass splitting (hydraulic fracturing)	Water inrush peak 3000 m^3/h	Grouting reinforcement
Huajiaoqing Tunnel (China)	Weathered rock	F-W	Tunnel face disintegration (hydraulic fracturing)	Water inrush m^3/d	Curtain grouting reinforcement
Daliang Tunnel (China)	Weatheredk rock	F-W	The arch of the tunnel face fell off (formation collapse)	10,000 m^3/h	Grouting reinforcement
Maluqing Tunnel (China)	Jointed and fractured rock	K-W	Collapse occurred in the tunnel face (formation collapse)	Water inrush peak 3×10^5 m^3/h	Curtain grouting
Shati Tunnel (China)	Jointed and fractured rock	F-W	Jointed and fractured rock (hydraulic fracturing)	Tunnel face water inrush 9686 m^3/d	Grouting reinforcement
Yesanguan Tunnel (China)	Fractured fault zone	K-W	Fractured rock splitting (hydraulic fracturing)	Initial 30 min water inflow 15,100 m^3	Curtain grouting
Wulaofeng Tunnel (China)	Jointed and fractured rock	F-W	Rock disintegration (hydraulic fracturing)	peak value reached 980 m^3/h	Grouting reinforcement
Pingtian Tunnel (China)	Fractured fault zone	F-W	Surrounding rock fragmentation (formation collapse)	The water output reached 1000 m^3/h	Backfill concrete
Shengli Tunnel (China)	Fractured fault zone	F-W	Collapse of support structure (formation collapse)	The water output reached 2×10^6 m^3	Curtain grouting reinforcement
Dabieshan Tunnel (China)	Weathered rock	F-W	Groundwater washes away fissure filling (interface slip)	Continuous water inflow	Grouting reinforcement

Table 1. *Cont.*

Tunnel Name	Unfavorable Geology	Water Supply	Causes of Water Inrush	Water Inrush Scale	Reinforcement Measure
Geleshan Tunnel (China)	Fractured fault zone	K-W	Groundwater washed away the filling (interface slip)	Water inflow 80 m³/h	Curtain grouting to block water
Tongyu Tunnel (China)	Jointed and fractured rock	K-W	Filling destabilised by infiltration (formation collapse)	Collapse volume 5000 m³	Backfill concrete
Daxiangling Tunnel (China)	Fractured fault zone	F-W	Cracks developed (interface slip)	Water inflow 17,000 m³/d	Grouting reinforcement
Wuzhishan Tunnel (China)	Jointed and fractured rock	K-W	Rock mass splitting (hydraulic fracturing)	Peak water inrush 16,000 m³/d	Grouting reinforcement
Shijingshan Tunnel (China)	Strongly weathered rock	F-W	Weak rock fractured (hydraulic fracturing)	Continuous water inflow	Grouting
Huayingshan Tunnel (China)	Fractured fault zone	K-W	Groundwater washed away the filling (interface slip)	Continuous water inflow	Grouting reinforcement
Huinongshan Tunnel (China)	Fractured fault zone	F-W	Collapse and instability rock (formation collapse)	Water inflow 1676 m³/h	Grouting reinforcement
Shibanling Tunnel (China)	Fractured fault zone	F-W	Fracture opened (interface slip)	Water inflow 3500 m³/d	Grouting reinforcement
Shangpilin Tunnel (China)	Weathered rock mass	K-W	Collapse of cavern fill at tunnel face (formation collapse)	Water inrush inflow	CRD method
Xuefengshan Tunnel (China)	Fractured fault zone	F-W	Fracture opened(interface slip)	Continuous water inflow	Curtain grouting reinforcement
Kaoyishan Tunnel (China)	Weathered rock	F-W	Collapse (formation collapse)	Water gushing collapse	Grouting reinforcement
Guanyinyan Tunnel (China)	Fractured fault zone	F-W	Flow took away fine particles (interface slip)	Water inrush 1080 m³/h	Backfill concrete
A river tunnel(China)	Jointed and fractured rock	R-W	Leakage of pipe joints (interface slip)	Seepage accumulated for 30 m	High pressure grouting
A water conveyance tunnel (China)	Jointed and fractured rock	R-W	Deformation of pipe segments (interface slip)	Water inrush of single well 1600 m³/d	Freezing method
Jiaozhou Bay Tunnel (China)	Jointed and fractured rock	S-W	Splitting of primary fractures (hydraulic fracturing)	Water gushing behind the initial branch	Grouting reinforcement
Xiang'an Tunnel (China)	Strongly weathered rock	S-W	Excavation unloading (interface slip)	Continuous seepage	Grouting reinforcement
Seikan Tunnel (Japan)	Fractured fault zone	S-W	Separation of grouting body (formation collapse)	Peak water inflow 5100 m³/h	Full-face grouting reinforcement
Atlantic Ocean Tunnel (Norway)	Fractured fault zone (cave-in)	S-W	Fractured rock collapsed (formation collapse)	Single borehole up to 500 L/min	Grouting reinforcement
Hanekleiv Tunnel (Norway)	Jointed and fractured rock	S-W	Spalling failure of supporting structure (interface slip)	Continuous water inflow	Backfill concrete
Oslofjord Tunnel (Norway)	Jointed and fractured rock	S-W	Fractured rock mass (hydraulic fracturing)	Continuous water inflow	Freezing method
Bjory Tunnel (Norway)	Fractured fault zone	S-W	Seawater seepaged (interface slip)	Inflow 200 L/min	Grouting reinforcement
Ellingsy Tunnel (Norway)	Fractured fault zone	S-W	Fractured rock mass (formation collapse)	Inflow 400 L/min	Backfill concrete
Vardo Tunnel (Norway)	Fractured fault zone	S-W	Jointed and fractured rock (formation collapse)	Inflow 400 L/min	Grouting reinforcement
Karmsund Tunnel (Norway)	Fractured fault zone	S-W	Jointed and fractured rock (formation collapse)	Inflow 320 L/min	Grouting reinforcement
Godoy Tunnel (Norway)	Fractured fault zone	S-W	Presence of adverse principal stresses (interface slip)	Inflow 300 L/min	Grouting reinforcement
Slemmestad Tunnel (Norway)	Jointed and fractured rock	S-W	Jointed and fractured rock (formation collapse)	-	Grouting reinforcement
Vollsfjord Tunnel (Norway)	Jointed and fractured rock	S-W	Jointed and fractured rock (formation collapse)	-	Grouting reinforcement

Table 1. *Cont.*

Tunnel Name	Unfavorable Geology	Water Supply	Causes of Water Inrush	Water Inrush Scale	Reinforcement Measure
Byfjord Tunnel (Norway)	Fractured fault zone	S-W	Disintegration of the tunnel face (formation collapse)	Continuous seepage	Grouting reinforcement
Old Tanner Tunnel (Japan)	Fractured fault zone	S-W	Unstable surrounding rock (hydraulic fracturing)	Peak water inflow 134.4 m³/min	Grouting reinforcement
Channel Tunnel (UK–France)	Jointed and fractured rock	S-W	Jointed and fractured rock (hydraulic fracturing)	Continuous water inflow	Grouting reinforcement
Storebaelt Tunnel (Denmark)	Broken zone	S-W	Fractured rock splitting (hydraulic fracturing)	Super large water inrush submerged tunnel	Freezing method
Okayama subsea Tunnel (Japan)	Jointed and fractured rock	S-W	Fractured rock collapsed (formation collapse)	Continuous water inflow	-
Fossmark project Tunnel (Norway)	Jointed and fractured rock	F-W	Joints and fissures developed (hydraulic fracturing)	Inflow 0.4 L/s	Grouting reinforcement

Note: F-W: fissure water; K-W: Karst water; S-W: sea water; R-W: river water. The tunnel location in the table is indicated, and the tunnels mentioned below are no longer indicated.

4.2. Analysis of Water Inrush Characteristics

In the considered tunnels, from the perspective of water inrush volume, in a small event the water flow in a single crack was only 0.014~0.45 L/s (Xuefengshan Tunnel), and in a large event the water flow in a single borehole was up to 500 L/min (Atlantic Ocean Tunnel). The difference is very significant, showing the seriousness of the consequences of water inrush in a tunnel.

So far, there is lack of research on the classification criteria of water inrush for post-disaster in tunnels, and research has mostly focused on Karst tunnels, with almost none on subsea tunnels. By reviewing a large amount of literature, this paper extracts the classification criteria of the literature, as shown in Table 2 [62], Table 3 [63] and Table 4 [64]. From Tables 2–4, it can be seen that the classification of karst tunnel disaster level is mostly divided by the indicators of water inrush volume, mud volume, and instantaneous water pressure. In fact, the water pressure in submarine tunnels is large, and the water inrush process is often accompanied by large-scale collapse of the surrounding rock, which is fast and fierce, and the water volume is large. Therefore, the above criteria were optimized in combination with a subsea tunnel design code to propose a more consistent classification standard for underwater tunnels, as shown in Table 5 [65,66]. Two indicators, water inrush volume and collapse scale, were selected to evaluate the severity of water inrush hazard.

Reviewing Tables 1 and 5, among the three unfavorable geological features where water inrush occurs, a fault fracture zone is the most coming water inrush hazard, account for 46.5% (Figure 8). Water inrush is often accompanied by hydraulic fracturing, with a large water inrush. Due to the complexity of the geological conditions of the fault fracture zone, the distribution of water inrush of each level is relatively even (Figure 9a). In such unfavorable geology, 90% of the tunnels in jointed rock have large to extra-large water inrush accidents (Figure 9b), which are highly disastrous. Among them, the water inrush caused by tunnel collapse is mostly super-large, and the water inrush caused by interface slip is mostly of the general type. Weathered rock mass events are generally dominated by tunnel collapse or interface slip, in which large-scale water inrush disasters are related to tunnel collapse, while interface slip leads to water inrush mainly of general and small types (Figure 9c). The water inrush distribution of mountain tunnels is average, distributed at all levels, of which small disasters account for only 4.5%. The water inrush of subsea tunnels accounts for 36.8% of the extra-large hazards, which are disastrous, face a high water inrush risk, and the probability of general and small water inrush is also high (Figure 10).

Table 2. Updated size classification for water and mud/rock inrush in Karst tunnels.

Size Class	Size Description	Water Flux Range (m^3/h)	Mud/Rock VOLUME Range (m^3)
1	Small	$<1 \times 10^2$	$<1 \times 10^2$
2	Moderate	1×10^2 to 1×10^3	1×10^2 to 1×10^3
3	Large	1×10^3 to 1×10^4	1×10^3 to 1×10^4
4	Extremely large	$>1 \times 10^4$	$>1 \times 10^4$

Table 3. Classification of water bursts based on water volume.

Size Class	Water Inflow Q/(m^3/h)	Explanation (Water Pressure)
A	>10,000	Water inrush type: >0.5 Mpa
B	1000 to 10,000	Gushing, inrush type: <0.5 Mpa
C	100 to 1000	Gushing type: small water pressure does not affect construction
D	10 to 100	Groundwater flows slowly to meet drainage requirements

Table 4. Classification of water inrush in Karst tunnels.

Size Class	Water Flux Range (m^3/h)
I	>10,000, large water and mud inrush
II	3000 to 10,000, moderate water and mud inrush
III	500 to 3000, small water and mud inrush
IV	<500, fissures seepage

Table 5. Hazard classification.

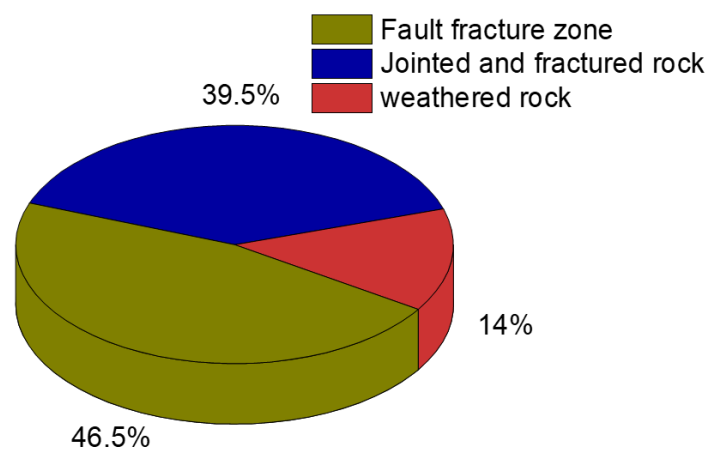| Classification of Water Inrush	Water Inflow (Q)	Collapse Volume
A (Extra large)	$Q > 5 \times 10^4$ m^3/d	Large amount of collapse or through the roof
B (large)	0.5×10^4 m^3/d $< Q < 5 \times 10^4$ m^3/d	Large collapse
C (General)	$Q < 0.5 \times 10^4$ m^3/d	Small collapse
D (small)	Small water inflow	——

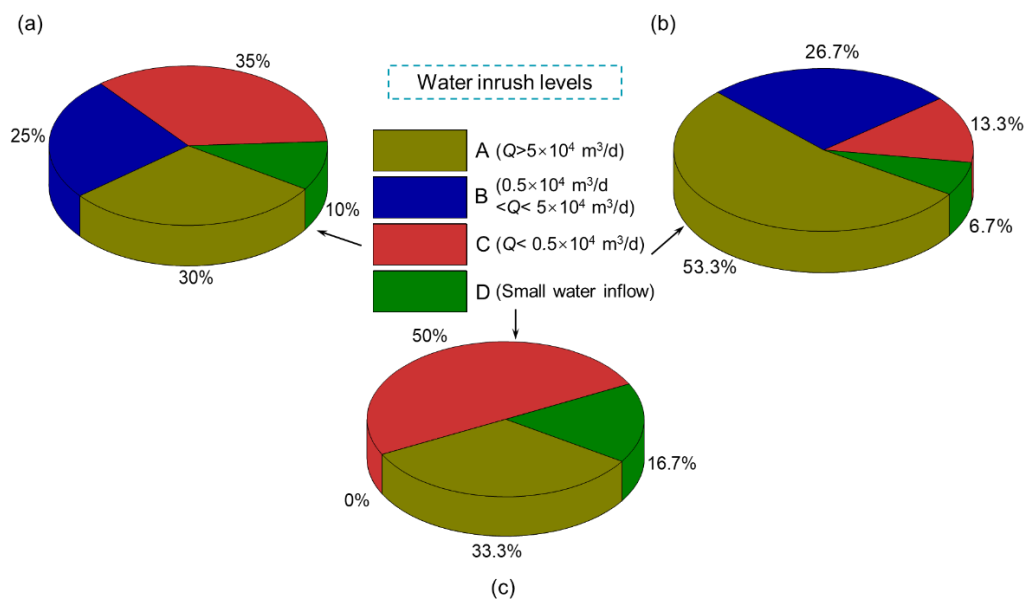**Figure 8.** Proportion of water inrush from each unfavorable geology type in tunnels.

Figure 9. Water inrush level distribution of three kinds of unfavorable geology in tunnels. (**a**) Fault fracture zone; (**b**) jointed and fractured rock; (**c**) weathered rock.
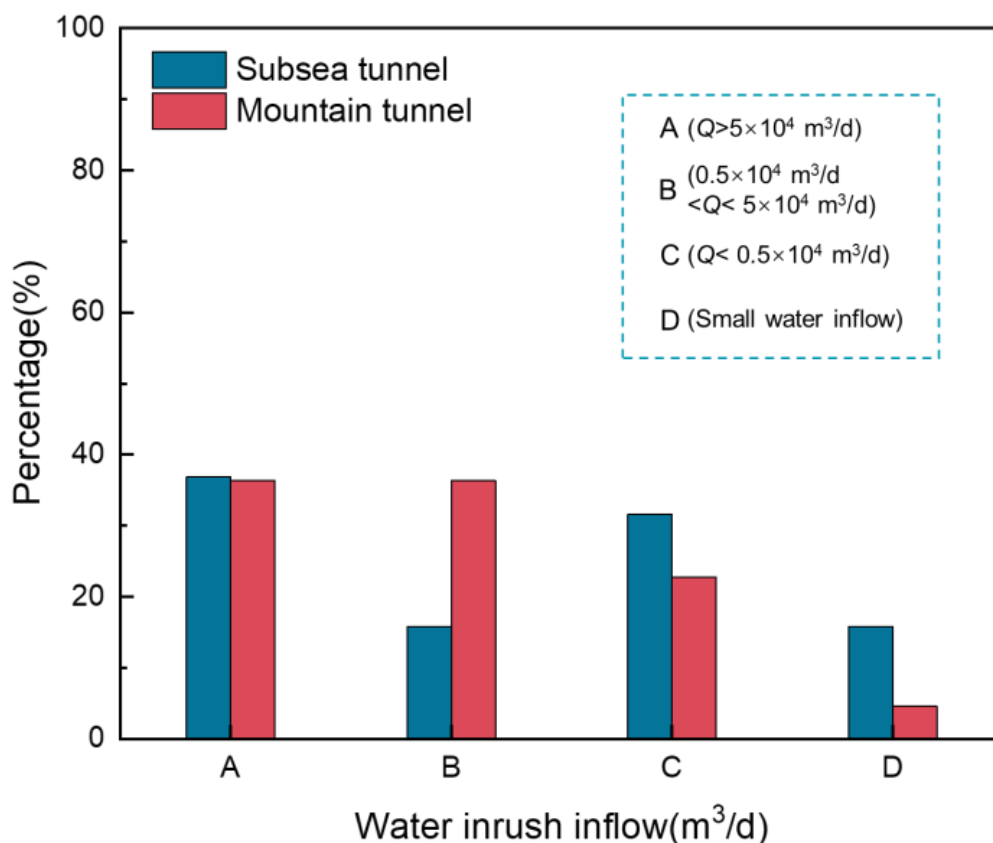

Figure 10. Percentage of water inrush inflow of subsea tunnels and mountain tunnels.

4.3. Water Inrush Modes

The mechanical mechanisms of the formation of water inrush passages, combined with water supply and permeation mechanisms, are divided into three modes: hydraulic fracturing, formation collapse, and interface slip, as shown in Figure 11.
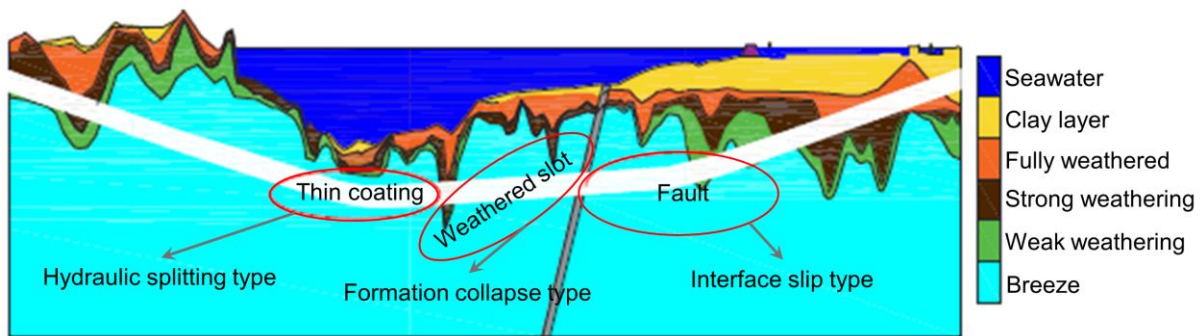
Figure 11. Water inrush modes [67].

4.3.1. Hydraulic Fracturing Type

Recently, a lot of research has been carried out on the high-pressure hydraulic fracturing of tunnels in terms of theoretical analysis, numerical simulation and field tests. Damage and fracture mechanics and catastrophe theory [67–72] were used to explore the relationship between rock failure modes and mechanical field. According to the crack propagation law of rock under different stress states, the formation mechanism of water inrush channel in the process of hydraulic fracturing was obtained. In terms of numerical simulation, the water inrush analysis of the Yuanliangshan Tunnel [73,74] showed that the surrounding rock was mechanically damaged under the action of hydraulic pressure, and the cracks expanded to form a channel, resulting in a water inrush hazard. Similarly, during the excavation of the Oslo-fjord Tunnel [75], a glacier erosion channel filled with high-permeability glacier sediments was encountered. The fractured rock mass cracked along the pathway. Based on different mechanical models, Guo et al. [76] used numerical analysis to show the failure process of a rock mass under the influence of hydraulic fracturing, and reproduced the expansion form of cracks in a rock mass. Based on the tunnel formation deformation evolution law and numerical simulation, Zhang et al. [67] demonstrated the evolution process of hydraulic fracturing in a subsea tunnel, as shown in Figure 12. It can be seen that at the initial stage of tunnel excavation, the seabed settlement was basically symmetrically distributed, and the settlement above the vault was the largest. As time progressed, due to the expansion of the cracking on the left side of the tunnel, the deformation of the surrounding rock on the left was greater than that on the right, and the seabed settlement curve presented an asymmetrical distribution. The variation law of vault settlement and seabed settlement with time was consistent. They both increased rapidly in the initial surrounding rock cracking stage, and the displacement rate decreased gradually after the expansion of cracking zone slowed down. Consequently, there was a correlation between vault settlement and seabed settlement.

In a field test, field water injection experiments were conducted based on the non-Darcy flow equation [77,78], and the expression between the permeability coefficient and the hydraulic pressure of the fractured rock mass was derived. This showed that the change of permeability coefficient can be used to determine whether the rock has hydraulic fracturing failure. As shown in Figure 13, the permeability coefficient increases rapidly when the hydraulic pressure reaches 4 MPa, and the mechanical damage of the rock increases, resulted in fracturing failure.

Based on the above research on the hydraulic fracturing characteristics of tunnels, the water inrush mechanism can be summarized as follows: due to the unloading of surrounding rock caused by tunnel excavation disturbance, a certain part around the tunnel produces splitting failure and gradually moves to the surface. If the thickness of overburden is small, the damaged area communicates with the surface, resulting in water inrush. When hydraulic fracturing water inrush occurs, the tunnel excavation usually does not expose the water bearing structure, but there is a relatively complete water barrier. This

has the following characteristics: high head pressure, large water inrush, high hazard, rock fracturing sound, and water mist is ejected on the rock wall.
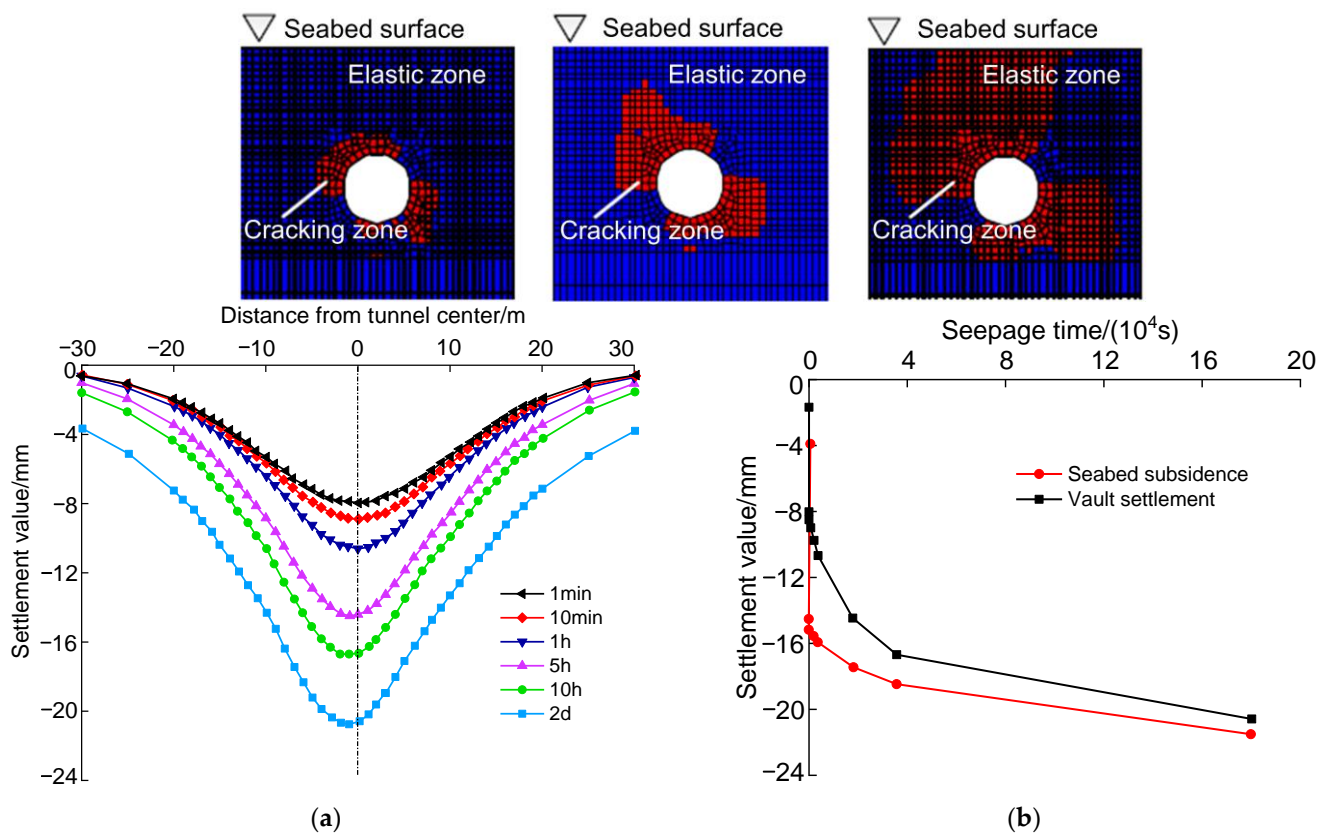

Figure 12. Evolution process and characteristics of hydraulic fracturing formations [67]. (**a**) Changes in seabed settlement; (**b**) corresponding relationship between seabed and dome settlement.
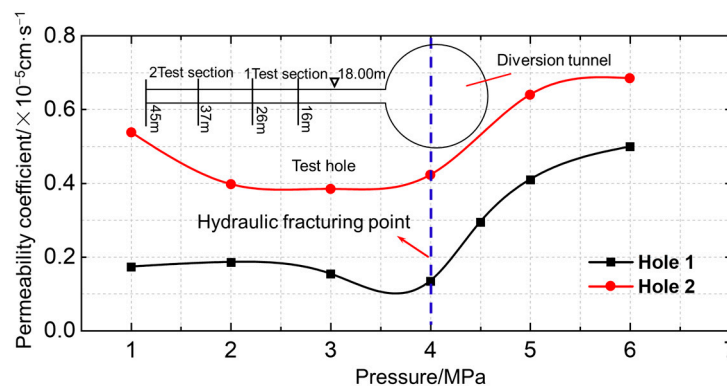

Figure 13. Relation curve between permeability coefficient and hydraulic pressure [77].

4.3.2. Formation Collapse Type

From the perspective of the permeability mechanism of a tunnel, through a combination of theoretical analysis and a numerical model Zhang [79] and Pan [54] divided formation deformation into four forms, i.e., excessive formation deformation, formation collapse, communication between formation interface and seawater, and permeability of formation filler. For instance, when the Seikan Tunnel [80] and the Tongyu Tunnel [81] crossed faults during construction, the grouting body was separated from the surrounding rock, and the stratum filler became permeable causing collapse. Related studies [82–86] have shown that tunnel construction through strongly weathered rock is highly susceptible to roofing and collapse causing destructive water inrush. During the excavation of the

Atlantic Ocean Tunnel [87], a progressive cavern was encountered, which contained a large amount of fissure water. As the tunnel face advanced, the fissure in the surrounding rock increased dramatically, and a 5–6 m high collapse occurred at the top of the tunnel covering the entire width and a 3 m circular length of the tunnel, as shown in Figure 14.

Figure 14. Collapse of the working face of Atlantic Ocean tunnel [87].

In the literature [57,88,89], based on the Pratt's theory using finite element software to perform an arithmetic analysis, the evolution of ground collapse damage caused by tunnel excavation is shown in Figure 15. Changes in the tunnel vault and seabed with time are consistent with the settlement evolution law. At 0~8 s, the settlement of the seabed and tunnel vault increased slowly with time. When the seepage time reached 8~10 s, corresponding to the previous stage of shear zone formation, the deformation rate began to increase in the later part of this stage. After the seepage time exceeded 10 s, a shear zone between the tunnel and the seabed gradually formed, the deformation rate increased rapidly, and eventually the surrounding rock collapsed.
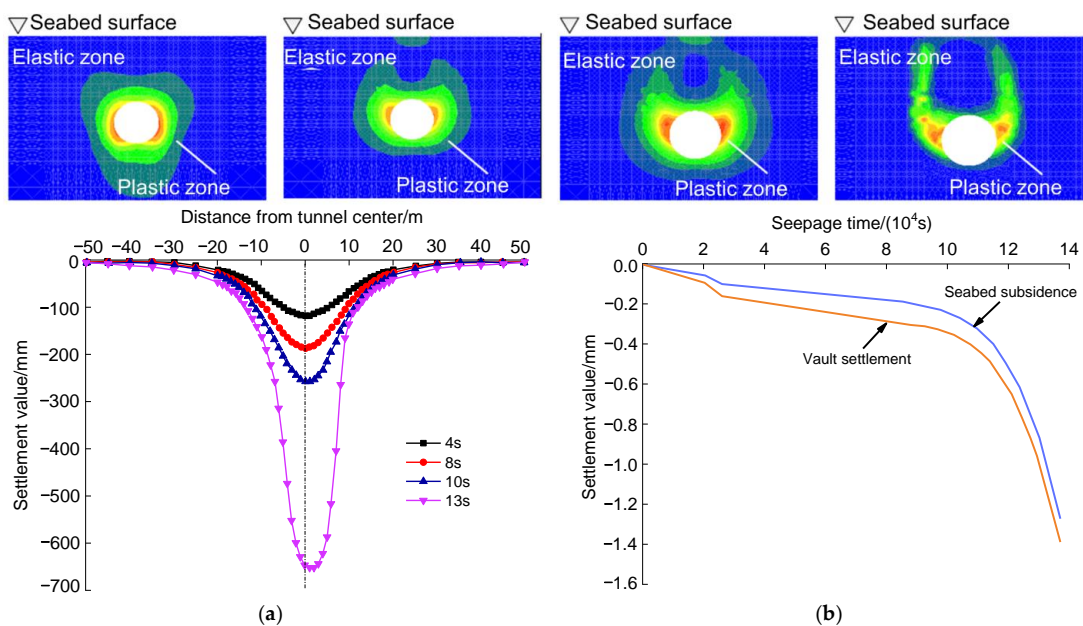

Figure 15. Evolution process and characteristics of the formation of collapsed ground [67]. (**a**) Changes in seabed settlement; (**b**) corresponding relationship between seabed and dome settlement.

The above research analyzes the mechanical characteristics and evolution process of formation collapse caused by unfavorable geology, and summarizes the water inrush mechanism as follows. Stress concentration caused by tunnel construction induces local instability or collapse of surrounding rock. If it is not treated in time, the collapse range continues to increase and extend to the seabed, resulting in the overall collapse of the formation. The strength and thickness of the water resisting layer decreases after the formation collapse, but not enough to resist the action of upper hydraulic pressure. Formation collapse has the following characteristics. At the beginning, the surrounding rock of the cave wall peels off or partially collapses. As the surrounding rock deforms, it gradually develops into an overall formation collapse, causing water inrush.

4.3.3. Interface Slip Type

Slip caused by the dislocation of surrounding rock was first based on key block theory [90–96]. Once the key block is unstable, several other blocks produce uncontrollable slip, which leads to formation of water inrush channels. Based on the cusp catastrophe theory, Song [66] and Xue et al. [97] established a structural plane sliding water inrush model with weak rock, obtaining the critical sliding surface length of structural plane sliding instability and proposed the interface opening mode. Taking the Xiang'an Tunnel and the Godoy Tunnel as examples, the surrounding rock excavation encountered water disintegration, which destroyed the original runoff conditions and eventually led to the occurrence of intrusion rock veins and bedrock contact interface gushing water. Research in [66,67] simulated the sliding failure caused by tunnel stratum dislocation based on the contact surface model and obtained the stratum change law in the process of interface sliding evolution. As shown in Figure 16, at 0~4 s, plastic deformation occurred in the formation, and the settlement of seabed and vault developed rapidly with time. At 4~14 s, the deformation rate was small, and the system energy was mainly dissipated in interface failure. When the seepage time reached 15 s, the whole interface was destroyed and slid, and the deformation increased suddenly. The excessive relative deformation caused the overall sliding of the structural plane, which marked the occurrence of interface sliding water inrush.
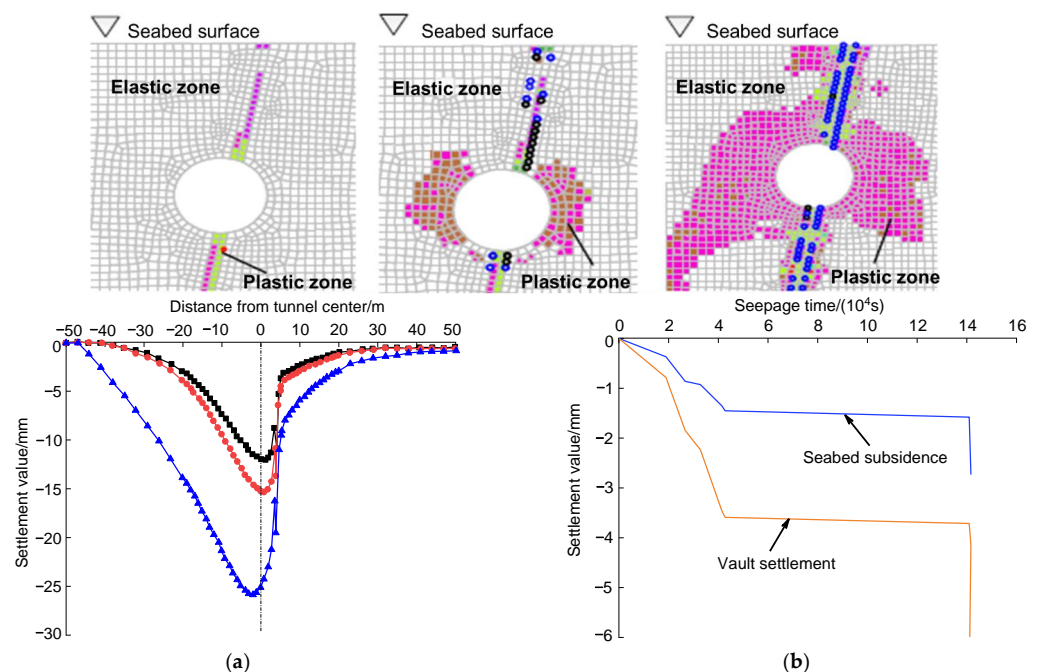

Figure 16. Evolution process and characteristics of interface slip formation [67]. (**a**) Changes in seabed settlement; (**b**) corresponding relationship between seabed and dome settlement.

The water inrush mechanism of interface sliding instability can be summarized as follows. When the buried depth of the tunnel is small, excavation and exposure of the aquifer can cause water seepage. If it is not treated in time, it develops and causes water inrush. Discontinuous deformation of the formation causes sliding of the structural plane, which can enhance its connectivity with the sea water and induce permeability of the tunnel. Stress change resulting from tunnel excavation causes the uneven deformation of the weak formation at the interface to produce shear or tension; however, formation strength at the interface is very low, so it is easy to cause formation damage and development, resulting in water permeability. Before the occurrence of interface slip water inrush, there are usually the following precursors. During tunnel construction, the structural surface of the surrounding rock is exposed, and there is usually a little water seepage or outflow along the structural surface, which gradually develops into water inrush.

5. Prevention and Treatment of Water Inrush Hazards Induced by Unfavorable Geology

5.1. Formation Reinforcement

The main problems of crossing a weak and unfavorable geological section of the seabed are reinforcement and water plugging [98–101]. To date, auxiliary construction methods often used in the engineering field include the grouting method, the freezing method and the backfilling concrete method. According to the statistical data in Section 4.1 and Figure 17, the most basic method is grouting reinforcement. For example, after water inrush occurred in the Jiaozhou Bay Tunnel and Xiang'an Tunnel, a grouting reinforcement method was used to block the developed cracks. For sections with complex geological structure and close hydraulic connection, the strength of rock and soil mass cannot meet construction requirements, and formation freezing is often required, such as in the water conveyance tunnel and the Oslo-fjord Tunnel. When the tunnel crosses fault fracture zones and other unfavorable geological features that may cause collapse, tunnel excavation can be used to the support structure and the rock mass. Loopholes need to be filled with backfill concrete, as in the Hanekleiv Tunnel and Ellingsy Tunnel.
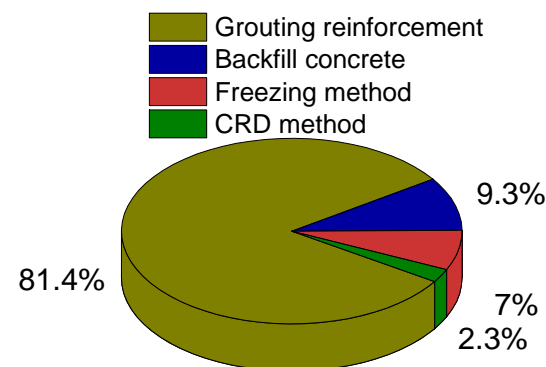

Figure 17. Proportions of formation reinforcement auxiliary construction methods.

(1)   Grouting reinforcement

Many studies have analyzed the mechanism of action of different grouting methods and proposed corresponding application conditions, but most have been aimed at a single grouting method [102–106] (Figure 18a). Because the traditional grouting method is the most empirical, performance and reliability of grouting plus solids is difficult to guarantee, and cases of water inrush due to grouting failure occur from time to time, such as in the Seikan Tunnel [107]. With the traditional single grouting method it is difficult to meet the performance index requirements of reliable formation reinforcement in unfavorable geological areas.
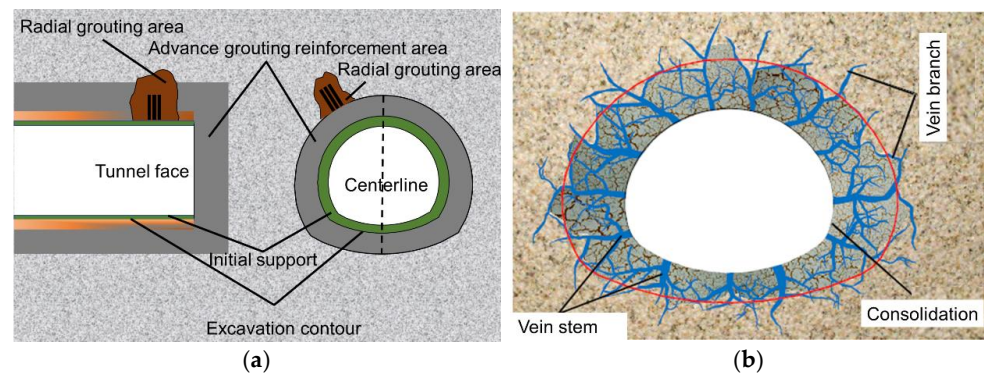
Figure 18. Comparison of grouting methods [103,108]. (**a**) Single full section crack grouting; (**b**) new concept of compound grouting.

A new concept of composite grouting has been proposed [108,109]. The mechanism of composite grouting adopts various methods and materials to improve the boundary conditions of engineering load, continuity, and integrity of stress transfer in a step-by-step manner (Figure 18b). Its essence is to form a functional composite structure through material compounding and process compounding to solve the problems of seepage resistance, strength, and stability of the strata, creating a functional composite structure-based tunnel perimeter curtain grouting technology. Compared with full section grouting, this has higher efficiency and more reliable performance, which has been verified in practical engineering applications in strong permeable sections. To effectively control the stability of surrounding rock in unfavorable geological areas and achieve a more satisfactory effect, grouting is carried out in four stages from the front of the excavation face to the completion of secondary lining construction. The specific grouting process is shown in Figure 19.

Figure 19. Processes of composite grouting [109]. (**a**) Advanced curtain grouting, (**b**) secondary reinforcement grouting, (**c**) localized infill grouting, (**d**) radial grouting.

Grouting also faces the problem of anti-corrosion and slurry material selection and ratio. How make grouting 100% effective without loss has become a hot topic. Seawater was filled with Cl^-, SO_2^{-4} and Mg^{2+} and other corrosive ions, which have an impact on the mechanical properties of grouting and the solid [110–113], resulting in the grouting body not being durable and subject to collapse. The selection of grouting protection materials for a tunnel [114–118] is related to the safety of tunnel construction. Different proportions of slurry and materials produce different mechanical effects, which have an important impact on water inrush protection. The project needs to ensure that the selected ratio of slurry and materials enhances the strength of the slurry.

(2)   Backfilled concrete

Water inrush is often accompanied by collapse. According to the formation mechanism and location of the collapse, choosing suitable materials and transportation methods to backfill concrete may achieve the expected reinforcement effect [119–123]. At first, rubble concrete, plain concrete and mortar rubble were the main materials used, but they were gradually eliminated due to their great weight and poor waterproof performance. Foamed concrete [124–126] is a lightweight filling material made by adding curing agent, water and air bubbles into the raw material (soil or sand) and fully mixing it (Figure 20). Foamed concrete has the characteristics of light weight, strength adjustable and high fluidity, and has been widely used in tunnels. For example, the Kolam Tunnel in Austria and the Dongtan Coal Mine Tunnel in China [127,128] used foamed concrete to absorb rock creep deformation, reducing the lining pressure, and thereby increasing the bearing capacity of the support structure to successfully solve the support problem (Figure 21). It can also be used to fill the cavity behind the lining, reducing the pressure transmitted to the lining by the surrounding rock, reducing backfill costs and providing a buffer phase for the deformation of the surrounding rock.
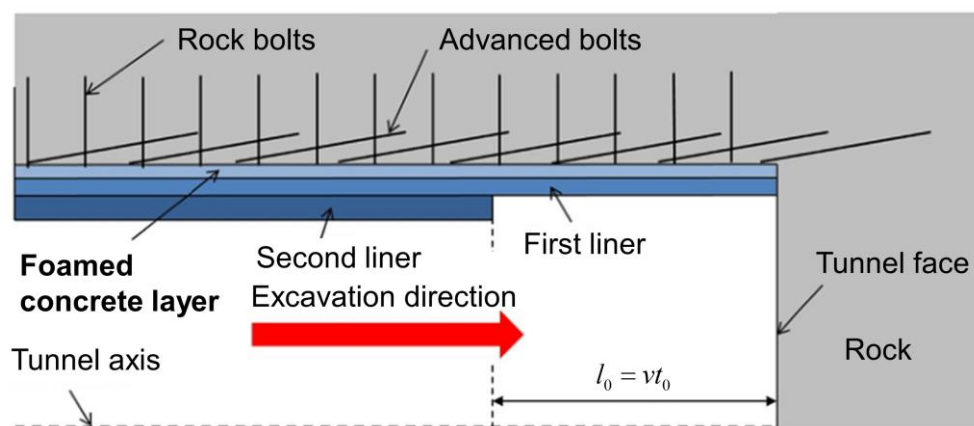

Figure 20. Applications of foamed concrete in tunnel support [125].

(3)   Artificial freezing method

Since the advent of the artificial freezing method, after decades of development, its theoretical system and construction technology have become more and more mature [129,130]. With its characteristics of environmental protection, low noise during construction, not occupying ground space, not affecting ground traffic and landscape, and little damage to the ground, it is widely used in tunneling projects. At present, it is mostly used in subway connection channel projects, shield import and export docking projects, and subway tunnel damage repair projects [131–135].
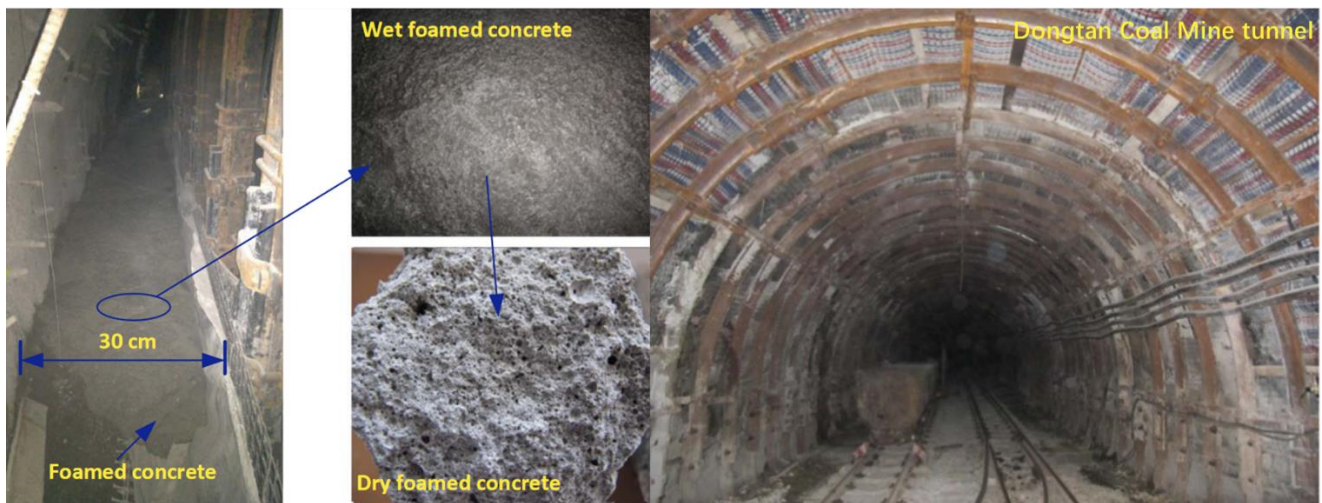
Figure 21. Applications of foamed concrete in the Duntan Tunnel [128].

The Tokyo Bay Tunnel in Japan and the Storebaelt Tunnel achieved shield by through ground freezing [136,137]. The early construction of the Shanghai Metro Line 2 [138] bypass and pumping station in China used horizontal freeze lining technology to ensure safe passage (Figure 22). The freezing method was adopted in the Beijing urban light rail section 14 crossing the north moat and Guangzhou Metro Line 2 [139] and crossing the fractured rock stratum near the Zhongshan Memorial Hall. The recently constructed Qiongzhou subsea Tunnel, Xiamen Metro Line 2 and Line 3 projects all used the freezing method to achieve safe construction of undersea tunnels with the aid of open chamber solutions.

Figure 22. Artificial freezing method application [138].

5.2. Optimization of Construction Method

The methods often used in subsea tunnel construction include the shield method, immersed method and drilling and blasting method [140]. The shield method [141–143] adopts modern production means, with high speed, high efficiency and a high degree of safety assurance. However, the flexibility of the tunneling mechanism is not large, the occupation ratio of equipment cost is high, and it is highly sensitive to geological conditions and suitable only for a soft soil layer. An immersed tunnel [144–146] has a low requirement for foundation bearing capacity, can be applicable to a variety of geological conditions and has good waterproof performance, but its working environment is poor, there are many processes involved with high cost, and this has a great impact on external shipping. Statistically [147–149], the drill-and-blast method accounts for more than 90% of the construction of submarine tunnels and has a wide range of applications, as in Norwegian tunnels, all of which have been constructed using this method. The drill-and-

blast method is relatively low cost and allows easy control of safety risks [150–152]. This section deals only with the optimization of this method in comparison to others.

Different construction methods [79,153,154] have a great impact on formation deformation and stability and selecting a reasonable construction scheme can effectively reduce formation deformation. A location with similar geological conditions should be selected for field tests to analyse the formation, deformation and structural forces during the tunnel construction process. Based on analysis of results a reasonable construction method can be determined.

For subsea tunnels constructed by the drilling and blasting method, the full-section method, the step method, the CRD method, and the double-side wall method are usually adopted. Generally speaking, under the same geological conditions, the construction speed of the full section method and the bench method are fast, and can be used for surrounding rock with favorable geological conditions; however, deformation is relatively large. The requirements for surrounding rock deformation control are extremely strict in tunnelling, so the above two methods are not applicable. CRD and the double-side wall method have a better effect on the control of formation settlement, but the construction speed is slower. In Figure 23, the horizontal displacement of using the double-side wall method is much larger than the corresponding value using the CRD method. Therefore, when using the double-side wall method, the horizontal support should be strengthened to effectively control horizontal deformation.
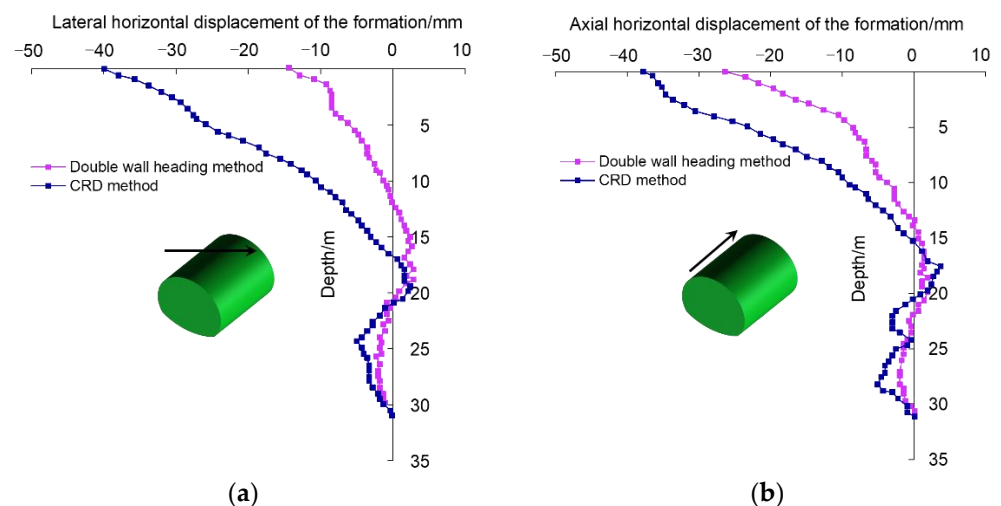

Figure 23. Horizontal displacement of the overlying ground of a tunnel [79]. (**a**) Lateral horizontal displacement of the formation; (**b**) axial horizontal displacement of the formation.

According to actual measurement results, the horizontal displacement during CRD construction was 20–50 mm (Figure 23), and the ground cracks were 1–15 mm (Figure 24). The horizontal displacement during the double-wall method construction was 40–70 mm, and the corresponding ground cracking was 1–30 mm. Therefore, the CRD method is more conducive to the control of formation cracking than the double sidewall method. For different rock conditions and water inrush modes, safety focus should be on comparing and analyzing the disturbance of each construction method on the surrounding rock. Selecting a reasonable construction method is very effective in controlling deformation of the surrounding rock.
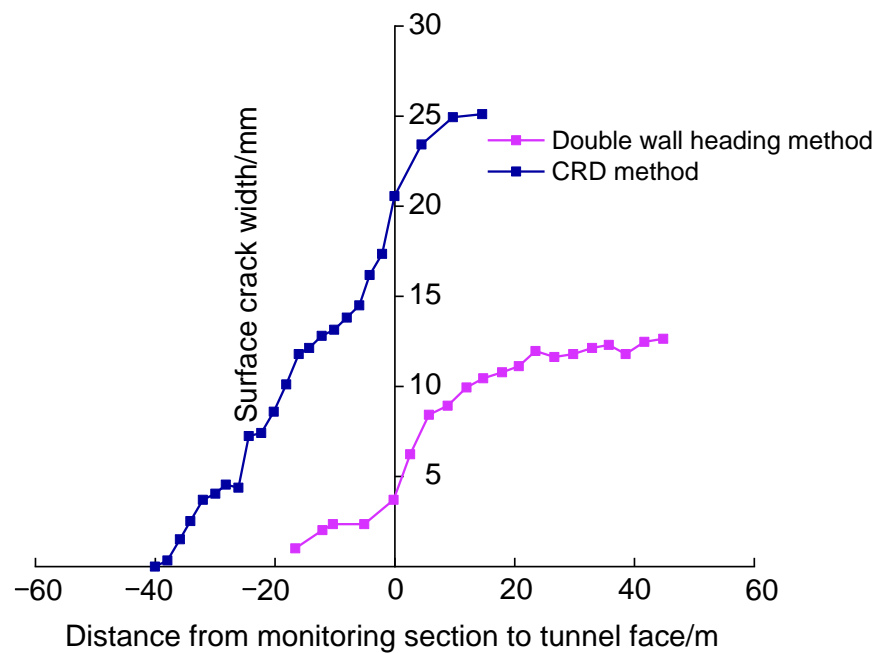
Figure 24. Surface crack propagation process curve [79].

5.3. Advanced Geological Prediction and Field Monitoring Technology

(1)　Advanced geological prediction

To determine the location, scale, shape and water volume of the structure in an un-excavated formation in front of a tunnel, advanced geological prediction has attracted much attention and has made great progress. Li et al. [24,155–161] has made outstanding contributions to the development of advanced geological prediction technology and its engineering applications. A transient electromagnetic method and ground penetrating radar are sensitive to water bearing geological structures, but they may be disturbed by the complex electromagnetic environment of the tunnel. At present, the transient electromagnetic method has made great progress in practical applications in terms of interpretation and observational devices [162,163], but it mainly focuses on two-dimensional detection, and its forward simulation and inverse interpretation in three-dimensional detection still need further research.

In practical engineering applications, projects that require advance forecasting should be determined according to the risk level of the tunnel section. Comprehensive selection of a variety of forecasting technologies should be conducted to ensure the accuracy and economy of advanced forecasting. Aiming at the high-risk water inrush section of a tunnel, a comprehensive quantitative advance geological prediction technology system for an entire subsea tunnel has been established [164] (Figure 25). This technical system has significantly improved the accuracy and reliability of forecasting and has been successfully applied to many projects [165]. However, it does not incorporate mutual constraint and substantive fusion between different types of detection information. To solve this problem, a joint inversion theory based on spatial structure constraints [166] was proposed, which is effective in multi-solution geophysical exploration. In the future, advance prediction technology of subsea tunnels should improve theoretical research, technology and equipment in the of automation, intelligence, quantification, refinement and real-time operation.
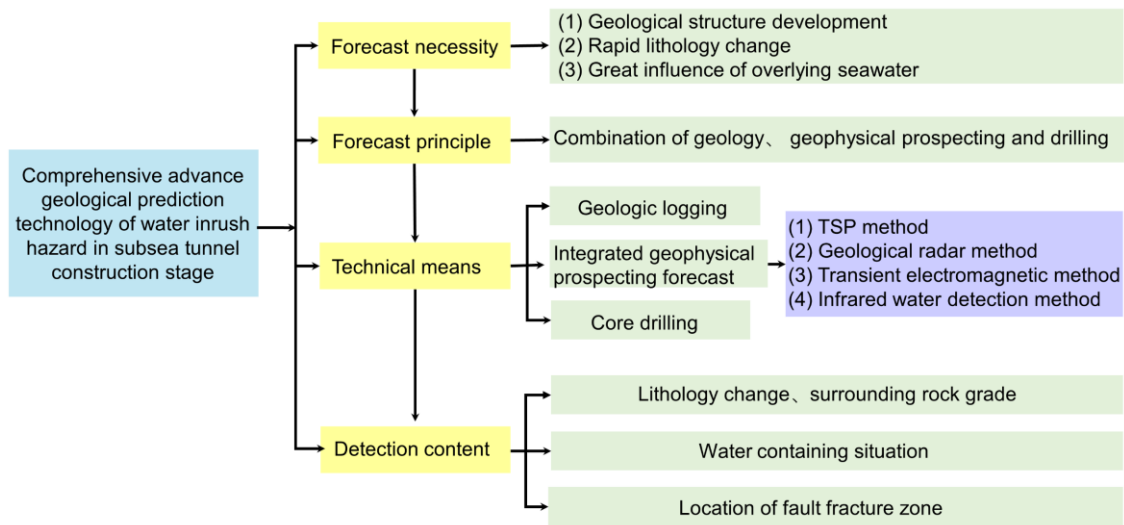
Figure 25. Comprehensive advanced geological prediction technology system for a subsea tunnel [164].

(2)   Formation deformation control method

Regardless of water inrush modes, inrush incubation, development and occurrence are accompanied by a continuous increase of stratum deformation [13,167–169]. According to the characteristics of water inrush evolution, the settlement and deformation rate of the tunnel vault are the main control indexes of water inrush risk. Corresponding to the three stages of the evolution of water inrush hazards, critical value of deformation in the corresponding stages is used as the control standard. Based on formation and deformation, a tunnel water inrush warning and alarm system has been established (Figure 26). U_n, U_a, and U_e are the critical deformation values during the incubation, development and formation stages of water inrush hazards. When actual settlement of the tunnel vault is $u < U_n$, the surrounding rock is still in an initial stable state, and construction can be carried out normally. When $U_n \leq u < U_a$, the surrounding rock begins to enter the failure stage, and deformation and damage are still under control, and increasing the monitoring frequency and taking necessary reinforcement and support measures to prevent the continuous deformation and damage of the surrounding rock should be implemented. When $U_a \leq u < U_e$, the deformation of the surrounding rock increases sharply, and damage rapidly develops and gradually enters an uncontrollable state. At this time, the variation trend of the surrounding rock deformation rate should be observed. When $u \geq U_e$, the tunnel may have water inrush at any time.
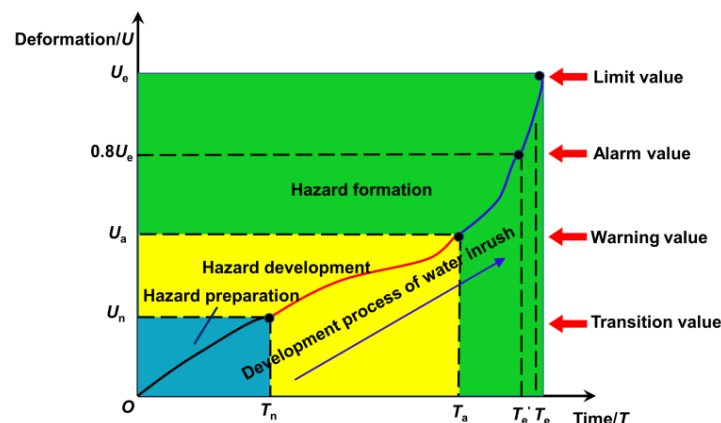

Figure 26. Early warning system for formation deformation [13].

To improve the reliability of the hazard management system, U_a is taken as the early warning value of water inrush, and 80% of the limit value U_e is taken as the alarm value, corresponding to different engineering prevention and control measures at different stages. However, this theory depends on real-time monitoring of formation deformation, and the data is complex and difficult to process.

(3)   Micro-Seismic Monitoring Method

Due to tunnel excavation and water pressure infiltration, the formation of water inrush channels and rock mass fracture is experienced in the process of macro crack initiation, propagation, penetration [170,171] This is accompanied by the release of energy in the form of seismic wave. The evolution of the water inrush process is always accompanied by strong micro-seismic activity [172,173]. At present, micro-seismic monitoring has been applied in the prevention and control of tunnel water inrush hazards. Qian [174] established the correlation between micro-seismic information and macroscopic activities of rock masses, revealing the mechanism of micro-seismic responses during the evolution of progressive damage and infiltration instability of rock masses and the filling media. Meanwhile, the scale and location of unfavorable geological features is delineated by seismic reflection wave technology [175,176], and the water-rich condition of the fault can be determined by combining the transient electromagnetic method. When water inrush occurs in the tunnel, the rock mass has dynamic characteristics of instability and failure, which can be used to evaluate the stability of the rock mass in the hazardous area. Chen [177] developed micro-seismic monitoring equipment for water inrush caused by fracture of the water-resisting rock mass in a tunnel and proposed a real-time monitoring scheme by observing structural failure of the water-resisting rock mass. A signal representing the water inrush fracture channel was obtained through practical application (Figure 27).
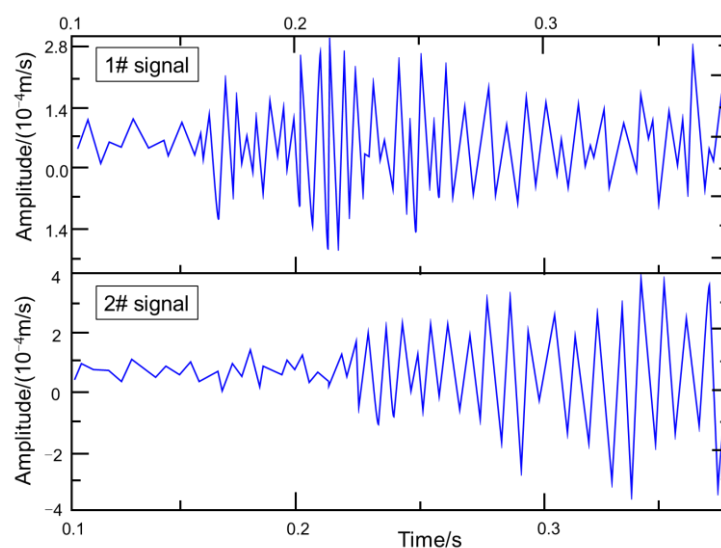
Figure 27. Micro-seismic signal of suspected water inrush channel rupture [177].

The rock mass may contain unfavorable geological structures such as joints, fissures and faults, which lead to the attenuation of seismic wave velocity and increase source positioning error. Although applying existing micro-seismic monitoring technology is an initial approach, the macro-precursor phenomenon of water inrush is not closely related to the micro-seismic field. Therefore, accurate acquisition of rock mass wave velocity field information is particularly important for accurate source positioning and geological prediction.

6. Discussion

In most cases, the occurrence of water inrush is related to the three types of unfavorable geology mentioned in Section 3.1, but it is also related to special geology such as Karst

caves [75]. Fault zones and jointed fissures contain a large number of developed Karst caves that can play an important role in the process of water inrush. In addition to being an area of protrusions, they are also a circulation area [37,38,49]. If they are extensively developed and connected to the seabed, solid-liquid mixtures can be introduced into the tunnel and a large-scale water inrush hazard can occur causing great harm. The Atlantic Ocean Tunnel is a typical case in which developed caves were associated with extreme expansion of fissures in the surrounding rock, which connected with the seabed to form a water inrush channel leading to massive collapse of the rock mass. Therefore, the position of water bearing structures should be accurately assessed in combination with advance geological prediction prior to tunnel excavation. The following is discussed in detail with respect to the ring breaking characteristics of subsea tunnel construction, waterproofing and drainage in three water inrush modes.

6.1. Difficulties in Subsea Tunnel Construction

Compared with "mountain tunnels", subsea tunnels have many obvious features in terms of engineering geology [75,178,179], such as difficulty in accurately surveying unfavorable geology, high drainage costs, and corrosive seawater. This, to a large extent, determines the complexity and high risk of a project (Figure 28).
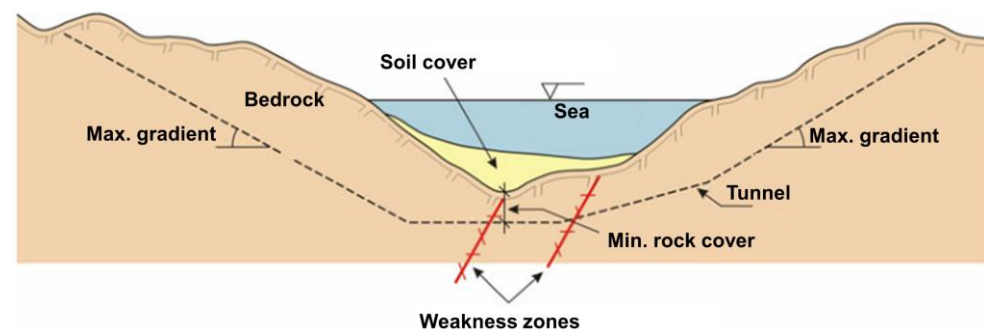

Figure 28. Typical longitudinal section of a subsea tunnel [75].

(1) Much of the project area is covered by water and, in most cases, there is a considerable soil cover on the sea floor. Special investigation techniques are required, and interpretation of the results is more uncertain than for most on-shore tunnel projects.

(2) The potential of water inflow is unknown, and the hydraulic pressure is often very high. In addition, all leakage water has to be pumped out of the descending tunnel.

(3) The locations of fjords and straits are, in most cases, defined by major faults or weakness zones in the bedrock. Even in good quality rock masses, the deepest part of the fjord, and thus the most critical part of the tunnel, often coincides with significant weakness zones representing very difficult ground conditions.

The cross-section of subsea tunnel usually has a "V"-shaped longitudinal slope. When a water inrush accident occurs in the unfavorable geological section of the tunnel, only manual pumping can be used, and the pumping cost and risk are relatively high. Relevant research [180–182] has shown that traditional structural waterproofing and drainage concepts ignore the water blocking effect and bearing capacity of the grouting reinforcement ring and initial support structure due to improper understanding of the role of support structure system. It is extremely dangerous to have an unclear understanding of this effect in unfavorable geological areas, where it easy to cause serious damage to the supporting structure. The traditional concept of waterproofing and drainage prevention of the structure in the past is no longer applicable, and it is necessary to establish an active control type of drainage prevention method (Figure 29) [20,183,184]. By actively adjusting the strength and seepage resistance of the surrounding rock reinforcement circle and the initial support structure, dual control of drainage and the force of the second lining structure can be realized. An active control waterproofing and drainage system is composed of a

"water blocking system" composed of the surrounding rock, a grouting reinforcement ring, the primary support and secondary lining, and a drainage system between the primary support and the secondary lining. By synergy between the active water blocking of the water blocking system and passive drainage of the drainage system, the water blocking and limiting drainage of the submarine tunnel is achieved. The essence of the system is the coordination of the plugging volume and the rational distribution of the water load, which includes synergy between the plugging system and the drainage system, synergy between the subsystems of the plugging system, and synergy between the parameters of the same plugging system.
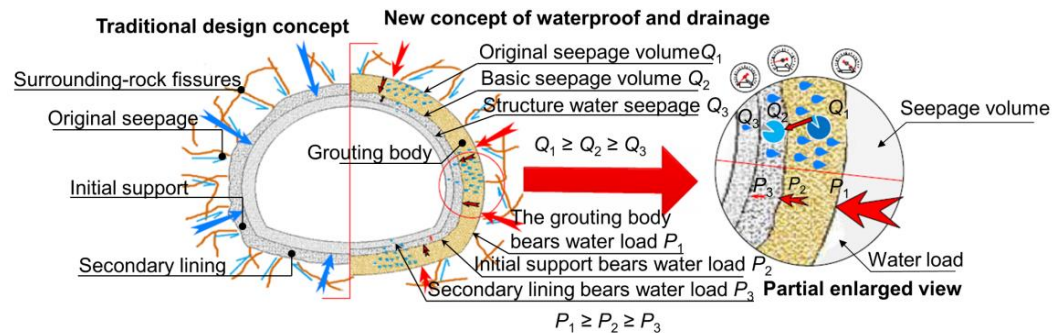

Figure 29. Comparison of waterproof drainage systems [183].

6.2. Comparison of Three Water Inrush Modes

The water inrush hazard of a tunnel is related to engineering the surrounding rock and communication of the rock damage area. Changes in surrounding rock deformation and seabed settlement with seepage time are related to three water inrush modes having phased characteristics. According to different water inrush modes, comparative analysis can be carried out with three aspects: the specific evolution process, formation deformation, and reinforcement measures, as shown in Tables 6 and 7. Combined with the evolution law of damage area of different water inrush modes, and the communication characteristics with seawater, the processes of water inrush can be divided into three stages, i.e., initial damage stage, damage developed stage, and hazard occurred stage.

Table 6. Characteristics of water inrush failure stages of different water inrush modes.

Water Inrush Mode	Initial Failure Stage		Destroy Sustainable Development Stage		Hazard Occurrence Stage	
Hydraulic fracturing	①	Surrounding rock is partially cracked;	①	Cracking area keeps increasing;	①	Cracked area communicates with the seabed to form a water inrush channel;
	②	Seabed subsidence is symmetrically distributed;	②	The deformation of formation and the seabed have an asymmetrical distribution;	②	Formation deformation continues to increase;
Formation collapse	①	Shear failure occurs around the caves;	①	Shear failure zone develops towards the seabed;	①	The formation of a shear-slip zone causes formation collapse;
	②	Settlement of the seabed and vault slowly develops with seepage time;	②	The formation deformation develops slowly, and the later deformation rate gradually increases;	②	The value and rate of stratum deformation increase sharply;
Interface slip	①	Plastic zone appears in the surrounding rock;	①	A plastic failure zone develops, and local shear failure occurs;	①	Plastic zone keeps increasing, leading to the overall slippage of the structural surface;
	②	Stratum deformation develops rapidly with the seepage time;	②	Formation deformation develops slowly;	②	The deformation of surrounding rock increases sharply.

Table 7. Percentage of reinforcement measures corresponding to different water inrush modes.

Water Inrush Modes	Ground Reinforcement Measures		
	Grouting Reinforcement	**Backfill Concrete**	**Artificial Freezing Method**
Hydraulic fracturing	84.6%	0%	15.4%
Formation collapse	80%	20%	0%
Interface slip	69.2%	23.1%	7.7%

As seen in Table 6, the deformation characteristics of the three water inrush modes are different at each stage. However, no matter the mode of water inrush, its hazard evolution process is manifested as a continuous increase in the deformation of the surrounding rock and strata. The uneven settlement of the seabed is the main cause of surface cracking and the formation of a water inrush channel. Studies in the past only focused on the deformation of the tunnel envelope and lacked research on the state of the seabed during construction [79]. In fact, the deformation of the seabed is much larger than the deformation of the tunnel envelope. It is important to control the safety of the tunnel by timely measurement of the rupture of the seabed [19]. Considering that it is difficult to accurately observe the seabed during the construction process, the deformation of the surrounding rock can be directly monitored [67]. Therefore, it is necessary to establish a dynamic quantitative relationship between the two according to the deformation propagation law of the overlying strata of the tunnel, i.e., to seek an indirect monitoring method. Through the control of surrounding rock deformation, the upper strata and seabed safety state are controlled, and the control standard of surrounding rock deformation is formulated. This can be broken down into different construction steps to obtain fine process control of unfavorable geological sections and ensure the safety of the whole construction process.

Table 7 shows that the characteristics of reinforcement measures corresponding to different water inrush modes are also different. The three water inrush modes relate to tunnels that have been grouted, but the hydraulic fracturing is more disastrous, and the proportion of stratum reinforcement by the artificial freezing method reaches 15.4%. The failure of stratum collapse and interface slip is accompanied by spalling and collapse of the surrounding rock. The proportion of the backfill concrete method is 20.0% and 23.1%, respectively. Different water inrush modes are generally dominated by one reinforcement measure, often accompanied by other measures, to assist reinforcement, resulting in a series of chain reactions that improve the stability of surrounding rock.

Grouting reinforcement, as the most commonly used reinforcement measure, accounts for a high percentage of the three water inrush modes. Combined with the new composite grouting process in Table 4 and Figure 17, the following section discusses different grouting schemes for different modes at different stages of development.

(1) For hydraulic fracturing, the cracks are filled with seawater immediately after they are formed. Under the action of hydraulic pressure, they expand and generate new branch cracks, causing adjacent cracks to connect and further connect the high-pressure water-rich zone and the tunnel front surface. The direction of the crack surface in the layer is analyzed for the position where hydraulic splitting may occur, and the corresponding weak position can be grouted for reinforcement without large-scale grouting.

(2) For formation collapse, the stratum conditions are generally poor, and the water damage caused is sudden and extremely harmful. Generally speaking, the following aspects should be considered for reinforcement. ① Curtain grouting or artificial freezing for preliminary reinforcement to avoid large-scale water inrush from collapse of the surrounding rock. ② Further improvement of the reinforcement effect of curtain grouting; ③ Backfill grouting behind the initial support and performing radial grouting in poor geological sections.

(3) For interface slip, when the surrounding rock conditions on both sides of the discontinuous structural plane or fracture zone are good, the overall instability of the tunnel will not be caused by structural plane sliding. Grouting reinforcement can

only be carried out for discontinuous structural planes or fracture zone areas. If the surrounding rock conditions on both sides of the discontinuous structural plane or the fracture zone are poor and may further cause stratum collapse, curtain grouting should be used for reinforcement.

Curtain grouting is widely used at present. However, in existing research, due to the lack of practical application guidance, there is less qualitative and quantitative research on curtain grouting. Therefore, it is important to optimize the grouting scheme based on the actual project combined with existing specifications to achieve dynamic grouting management as shown in Table 8. Four indicators of stratum conditions, maximum water output of the probe holes, water pressure, and sediment content in water are set based on advanced geological exploration data, thus dividing curtain grouting into three methods. Reasonable selection of grouting scheme can significantly reduce construction risk and improve construction efficiency.

Table 8. Curtain grouting schemes.

Grouting Schemes	Applicable Conditions			
	Stratum Conditions	Maximum Water Output of the Probe Hole/(m³/h)	Water Presure/Mpa	Sediment Content in Water/(kg/m³)
Full-face curtain grouting	Entire section is not self-stabilizing	≥20	≥0.3	≥100
Half-face curtain grouting	Local sections are not self-stabilizing	≥20	≥0.3	≥100
Perimeter curtain grouting	Surrounding soil is not self-stabilizing	≥10	≥0.2	≥10

7. Summary, Conclusions and Recommendations for Future Research

7.1. Summary and Conclusions

This paper represents a comprehensive review of research work on the hazards of water and mud inrush in subsea tunnels since the 1950s. In recent decades, academics have done a lot of research on the formation mechanism of water and mud inrush and have developed the most advanced technologies for mitigation measures for these kinds of hazards. Extensive efforts made by researchers have laid a solid foundation for the practical engineering application of advanced prediction and reinforcement techniques. However, there are still many unresolved research areas.

The unfavorable geology that causes water and mud inrush hazards can be divided into three categories. Statistical results show that the fault fracture zone, and jointed or fractured rock, are the most prone to intrusion of muddy water structures. Almost 86% of the hazards are caused by these two kinds of unfavorable geology. The strong weathering zone also plays a role in triggering water inrush hazards in submarine tunnels. The evolution of hazards depends not only on the construction method, but also on the location, size and shape of the hazard-causing structures adjacent to the tunnel. From the perspective of the formation mechanism of water inrush channels, three water inrush modes occur. The most effective method to reveal the hydraulic fracturing process of water inrush is the high-pressure water injection test on site, which enables observation of the formation process of the water inrush channel more intuitively and effectively. However, hydraulic splitting of water inrush under the action of multi-field coupling has not been solved and needs further research. In addition, the literature on water inrush caused by factors such as in-situ stress, earthquakes or blasting is quite limited, and there is an urgent need for research on these factors, especially for underwater tunnels with large, buried depths and large cross-sections.

At present, there are several monitoring technologies and treatment measures for prediction and prevention systems for water and mud inrush hazards. In particular, cement-bearing slurry structures can be identified and located through advanced geological prediction technology. Secondly, during construction, a section with similar geological conditions should be selected for field tests, and a reasonable construction method should

be determined based on the results of simulation software. At the same time, the evolution of a surrounding rock and water inrush channel can be monitored through formation deformation monitoring and micro-seismic monitoring technology, as well as using grouting technology, backfill concrete and artificial freezing to block water inrush channels. Finally, dynamic grouting can be used to block water with high flow velocity according to the evolution stage characteristics of the water inrush modes. The above hazard prevention methods and techniques have some weaknesses and require improvements.

7.2. Recommendations for Future Research

Based on this review, some topics may be identified for further research, as follows:

(1) In practical engineering, external factors such as earthquake, blasting, ground stress, and construction disturbance have an important influence on the occurrence of mud inrush disasters. However, the impact of external factors on the occurrence of adverse geological structures and mud inrush disasters is still unclear. Therefore, there is an urgent need to carry out research on the mechanism of mud inrush disasters and the criteria for disaster prevention, focusing on the multi-field coupling effects of water-earthquake-construction disturbance.

(2) It is recommended to actively combine artificial intelligence technology to improve the theoretical basis of geological structure identification and create three-dimensional-linkage identification technology. This technology can have different scales (cm-level to regional structures above 10 km), high-precision (cm-level 3D coordinates), and rapid and digital parameter measurement. Such research can provide a geological basis for the prediction and prevention of water and mud inrush disasters in tunnels.

(3) In disaster management, research on new automatic repair grouting materials and development of advanced intelligent grouting technology are of great significance for the prevention and treatment of water inrush hazards.

(4) The use the IoT and artificial intelligence technology combined with micro-seismic monitoring would be valuable to establish an intelligent early warning platform for remote water and mud inrush disasters. The system should have multiple functions, such as data collection, transmission, processing and early warning, which can accurately locate and monitor the rupture position of a water inrush channel.

References

1. Chen, J.; Feng, X.; Wei, H.; Feng, H. Statistics on Underwater Tunnels in China. *Tunnel. Constr.* **2021**, *41*, 483–516. (In Chinese)
2. Tsinidis, G.; de Silva, F.; Anastasopoulos, I.; Bilotta, E.; Bobet, A.; Hashash, Y.M.A.; He, C.; Kampas, G.; Knappett, J.; Madabhushi, G.; et al. Seismic behaviour of tunnels: From experiments to analysis. *Tunn. Undergr. Space. Technol.* **2020**, *99*, 103334. [CrossRef]
3. Li, S.; He, P.; Li, L.; Shi, S.; Zhang, Q.; Zhang, J.; Hu, J. Gaussian process model of water inflow prediction in tunnel construction and its engineering applications. *Tunn. Undergr. Space Technol.* **2017**, *69*, 155–161. [CrossRef]
4. Xue, Y.; Kong, F.; Li, S.; Qiu, D.; Su, M.; Li, Z.; Zhou, B. Water and mud inrush hazard in underground engineering: Genesis, evolution and prevention. *Tunn. Undergr. Space Technol.* **2021**, *114*, 103987. [CrossRef]
5. Song, Q.; Xue, Y.; Li, G.; Su, M.; Qiu, D.; Kong, F.; Zhou, B. Using Bayesian network and Intuitionistic fuzzy Analytic Hierarchy Process to assess the risk of water inrush from fault in subsea tunnel. *Geomech. Eng.* **2021**, *27*, 605–614. [CrossRef]
6. Zhang, P.; Huang, Z.; Liu, S.; Xu, T. Study on the Control of Underground Rivers by Reverse Faults in Tunnel Site and Selection of Tunnel Elevation. *Water* **2019**, *11*, 889. [CrossRef]
7. Qiu, D.; Chen, Q.; Xue, Y.; Su, M.; Liu, Y.; Cui, J.; Zhou, B. A new method for risk assessment of water inrush in a subsea tunnel crossing faults. *Mar. Geores. Geotechnol.* **2021**, *6*, 1–11. [CrossRef]
8. Zhang, N.; Zheng, Q.; Elbaz, K.; Xu, Y. Water inrush hazards in the Chaoyang Tunnel, Guizhou, China: A preliminary investigation. *Water* **2020**, *12*, 1083. [CrossRef]
9. Kong, H.; Zhao, L.; Zhang, N. Water Inrush Hazard in Shijingshan Tunnel during Construction, Zhuhai, Guangdong, China. *Safety* **2022**, *8*, 7. [CrossRef]
10. Song, J.; Chen, D.; Wang, J.; Bi, Y.; Liu, S.; Zhong, G.; Wang, C. Evolution Pattern and Matching Mode of Precursor Information about Water Inrush in a Karst Tunnel. *Water* **2021**, *13*, 1579. [CrossRef]
11. Zhang, G.; Jiao, Y.; Wang, H.; Chen, Y.; Chen, L. On the mechanism of inrush hazards when Denghuozhai Tunnel passing through granite contact zone. *Tunn. Undergr. Space Technol.* **2017**, *68*, 174–186. [CrossRef]
12. Li, S.; Wu, J.; Xu, Z.; Zhang, B.; Huang, X. Escape route analysis after water inrush from the working face during submarine tunnel excavation. *Mar. Geores. Geotechnol.* **2018**, *36*, 379–392. [CrossRef]
13. Zhang, D. Essential issues and their research progress in tunnel and underground engineering. *Chin. J. Theor. Appl. Mechanics.* **2017**, *49*, 3–21. (In Chinese)
14. He, S.; Lai, J.; Li, Y.; Wang, K.; Wang, L.; Zhang, W. Pile group response induced by adjacent shield tunnelling in clay: Scale model test and numerical simulation. *Tunn. Undergr. Space Technol.* **2022**, *120*, 104039. [CrossRef]
15. Hong, K. Typical underwater tunnels in the mainland of China and related tunneling technologies. *Engineering* **2017**, *3*, 871–879. [CrossRef]
16. Dammyr, O.; Nilsen, B.; Gollegger, J. Feasibility of tunnel boring through weakness zones in deep Norwegian subsea tunnels. *Tunn. Undergr. Space Technol.* **2017**, *69*, 133–146. [CrossRef]
17. Li, P.; Wang, F.; Zhang, C.; Li, Z. Face stability analysis of a shallow tunnel in the saturated and multilayered soils in short-term condition. *Comput. Geotech.* **2019**, *107*, 25–35. [CrossRef]
18. Li, S.; Li, P.; Zhang, M. Analysis of additional stress for a curved shield tunnel. *Tunn. Undergr. Space Technol.* **2021**, *107*, 103675. [CrossRef]
19. Shi, P.; Zhang, D.; Pan, J.; Liu, W. Geological investigation and tunnel excavation aspects of the weakness zones of Xiang'an subsea tunnels in China. *Rock Mech. Rock Eng.* **2016**, *49*, 4853–4867. [CrossRef]
20. Sun, Z.; Zhang, D.; Fang, Q. Determination method of reasonable reinforcement parameters for subsea tunnels considering ground reinforcement and seepage effect. *Appl. Sci.* **2019**, *9*, 3607. [CrossRef]
21. Xue, Y.; Qu, C.; Su, M.; Qiu, D.; Li, X.; Ma, X. Comprehensive and Quantitative Evaluation of Subsea Tunnel Route Selection: A Case Study on Bohai Strait. *KSCE J. Civ. Eng.* **2021**, *25*, 3540–3555. [CrossRef]
22. Shekari, M. A coupled numerical approach to simulate the effect of earthquake frequency content on seismic behavior of submarine tunnel. *Mar. Struct.* **2021**, *75*, 102848. [CrossRef]
23. Yang, W.; Fang, Z.; Yang, X.; Yang, X.; Shi, X.; Wang, J.; Wang, H.; Bu, L.; Li, L.; Zhou, Z.; et al. Experimental study of influence of karst aquifer on the law of water inrush in tunnels. *Water* **2018**, *10*, 1211. [CrossRef]
24. Li, S.; Liu, C.; Zhou, Z.; Li, L.; Shi, S.; Yuan, Y. Multi-sources information fusion analysis of water inrush disaster in tunnels based on improved theory of evidence. *Tunn. Undergr. Space Technol.* **2021**, *113*, 103948. [CrossRef]
25. Tu, W.; Li, L.; Cheng, S.; Chen, D.; Yuan, Y.; Chen, Y. Evolution Mechanism, Monitoring, and Early Warning Method of Water Inrush in Deep-Buried Long Tunnel. *Geofluids* **2021**, *2021*, 2023782. [CrossRef]
26. Huang, Z.; Zeng, W.; Wu, Y.; Li, S.; Zhao, K. Experimental investigation of fracture propagation and inrush characteristics in tunnel construction. *Nat. Hazards* **2019**, *97*, 193–210. [CrossRef]
27. He, X.; Zhou, X.; Xu, Y.; Ma, T.; Wu, T. Study on the Influence of Nonlinear Seepage and Grouting Reinforcement on Surrounding Rock in Subsea Tunnel. *J. Coast. Res.* **2020**, *111*, 162–167. [CrossRef]
28. Li, S.; Zheng, Z.; Liu, R.; Wang, X.; Zhang, L.; Wang, H. Analysis on fracture grouting mechanism considering grout-rock coupling effect. *Chin. J. Rock Mech. Eng.* **2017**, *36*, 812–820. (In Chinese)
29. Jiang, Z.; Pan, D.; Zhang, S.; Yin, Z.; Zhou, Z. Advanced Grouting Model and Influencing Factors Analysis of Tunnels with High Stress and Broken Surrounding Rock. *Water* **2022**, *14*, 661. [CrossRef]

30. China National Knowledge Infrastructure (CNKI). Available online: https://www.cnki.net/ (accessed on 27 April 2022).

31. Elsevier ScienceDirect. Available online: https://www.sciencedirect.com/ (accessed on 27 April 2022).

32. Springer Link, Springer Nature. Available online: https://link.springer.com/ (accessed on 27 April 2022).

33. Engineering Index, Engineering Information Inc. Available online: https://www.engineeringvillage.com/ (accessed on 27 April 2022).

34. Web-of-Science, Clarivate Analytics. Available online: https://clarivate.com/products/web-of-science/ (accessed on 27 April 2022).

35. Taylor & Francis-Online, Taylor & Francis Group. Available online: https://www.tandfonline.com/ (accessed on 27 April 2022).

36. ASCE-Library, American Society of Civil Engineers. Available online: https://ascelibrary.org (accessed on 27 April 2022).

37. Nilsen, B.; Palmstrφm, A. Stability and Water Leakage of Hard Rock Subsea Tunnel. In *Modern Tunneling Science and Technology*; Routledge: London, UK, 2017; pp. 497–502.

38. Nilsen, B. Analysis of potential cave-in from fault zones in hard rock subsea tunnels. *Rock Mech. Rock Eng.* **1994**, *27*, 63–75. [CrossRef]

39. Shin, J.; Choi, K.C.; Yoon, J.U.; Shin, Y. Hydraulic significance of fractured zones in subsea tunnels. *Mar. Geores. Geotechnol.* **2011**, *29*, 230–247. [CrossRef]

40. Li, Y. *Key Technology Study on Qingdao Jiaozhou Bay Subsea Tunnel Crossing Seabed Fault Zone*; Beijing Jiaotong University: Beijing, China, 2017. (In Chinese)

41. Nilsen, B. Main challenges for deep subsea tunnels based on norwegian experience. *J. Korean Tunn. Undergr. Space Assoc.* **2015**, *17*, 563–573. [CrossRef]

42. Mao, D.W.; Nilsen, B.; Lu, M. Numerical analysis of rock fall at Hanekleiv road tunnel. *Bull. Eng. Geol. Environ.* **2012**, *71*, 783–790. [CrossRef]

43. Zhao, Y.; Peng, Q.; Wan, W.; Wang, W.; Zhang, S. Seepage-fracture coupling mechanism of rock masses cracking propagation under high hydraulic pressure and numerical verification. *Rock Soil Mech.* **2014**, *35*, 556–564. (In Chinese)

44. Huang, Y.; Zhou, Z.; Fu, S.; Hu, D.; Li, S. Study on variation of rock mass permeability with high pressure permeability test. *J. Eng. Geol.* **2013**, *21*, 828–834. (In Chinese)

45. Xiong, L.; Zhang, D.; Zhang, Y. Water leakage image recognition of shield tunnel via learning deep feature representation. *J. Vis. Commun. Image Represent.* **2020**, *71*, 102708. [CrossRef]

46. Li, Z.; Lai, J.; Li, Y.; Qiu, J.; Shi, Y.; Li, B.; Fan, F. Ground fissure disasters and mitigation measures for hazards during metro system construction in Xi'an, China. *Arab. J. Geosci.* **2022**, *15*, 1–16. [CrossRef]

47. Ma, E.; Lai, J.; Xu, S.; Shi, X.; Zhang, J.; Zhong, Y. Failure analysis and treatments of a loess tunnel being constructed in ground fissure area. *Eng. Fail. Anal.* **2022**, *134*, 106034. [CrossRef]

48. Xu, S.; Ma, E.; Lai, J.; Yang, Y.; Liu, H.; Yang, C.; Hu, H. Diseases Failures Characteristics and Countermeasures of Expressway Tunnel of Water-rich Strata: A Case Study. *Eng. Fail. Anal.* **2022**, *134*, 106056. [CrossRef]

49. Xue, Y.; Zhou, B.; Li, S.; Qiu, D.; Zhang, K.; Gong, H. Deformation rule and mechanical characteristic analysis of subsea tunnel crossing weathered trough. *Tunn. Undergr. Space Technol.* **2021**, *114*, 103989. [CrossRef]

50. Zhou, B. *Study on Water Inrush Mechanism and Risk Evaluation of Subsea Tunnel Crossing Weathered Trough*; Shandong University: Jinan, China, 2019. (In Chinese)

51. Zhang, W.; Lai, T.; Li, Y. Risk Assessment of water supply network operation based on anp-fuzzy comprehensive evaluation method. journal of pipeline systems engineering and practice. *J. Pipeline Syst. Eng. Pract.* **2022**, *13*, 04021068. [CrossRef]

52. Ma, F.; Zhao, H.; Guo, J. Investigating the characteristics of mine water in a subsea mine using groundwater geochemistry and stable isotopes. *Environ. Earth Sci.* **2015**, *74*, 6703–6715. [CrossRef]

53. Zhou, W.; Liao, S.; Men, Y. A fluid-solid coupled modeling on water seepage through gasketed joint of segmented tunnels. *Tunn. Undergr. Space Technol.* **2021**, *114*, 104008. [CrossRef]

54. Pan, J. *Stability Analysis and Control of Rock Mass During Subsea Tunneling in Unfavorable Geological Conditions*; Beijing Jiaotong University: Beijing, China, 2016. (In Chinese)

55. Wu, J. *Expansion of Water Inrush Channel, Minimum Rock Thickness and Escape Routes Optimization of Karst Tunnel*; Shandong University: Jinan, China, 2018. (In Chinese)

56. Liu, J.; Li, Z.; Zhang, X.; Weng, X. Analysis of Water and Mud Inrush in Tunnel Fault Fracture Zone—A Case Study of Yonglian Tunnel. *Sustainability* **2021**, *13*, 9585. [CrossRef]

57. Du, Y.; Liu, W.; Meng, X.; Pang, L.; Han, M. Effect of Crack Propagation on Mining-Induced Delayer Water Inrush Hazard of Hidden Fault. *Geofluids* **2021**, *2021*, 6557578. [CrossRef]

58. Huang, Z.; Zhao, K.; Li, X.; Zhong, W.; Wu, Y. Numerical characterization of groundwater flow and fracture-induced water inrush in tunnels. *Tunn. Undergr. Space Technol.* **2021**, *116*, 104119. [CrossRef]

59. Zhou, J.; Wei, J.; Yang, T.; Zhang, P.; Liu, F.; Chen, J. Seepage channel development in the crown pillar: Insights from induced microseismicity. *Int. J. Rock Mech. Min. Sci.* **2021**, *145*, 104851. [CrossRef]

60. Qin, Y.; Qiu, J.; Lai, J.; Liu, F.; Wang, L.; Luo, Y.; Liu, T. Seepage Characteristics in Loess Strata Subjected to Single Point Water. *Suppl. J. Hydrol.* **2022**, *609*, 127611. [CrossRef]

61. Wu, J.; Jia, C.; Zhang, L. Expansion of water inrush channel by water erosion and seepage force. *Int. J. Geomech.* **2021**, *21*, 04021121. [CrossRef]

62. Xue, Y.; Kong, F.; Qiu, D.; Su, M.; Zhao, Y.; Zhang, K. The classifications of water and mud/rock inrush hazard: A review and update. *Bull. Eng. Geol. Environ.* **2021**, *80*, 1907–1925. [CrossRef]

63. Li, X.; Zhang, D.; Fang, Q.; Song, H. On water burst patterns in underwater tunnels. *Mod. Tunnel. Technol.* **2015**, *52*, 24–31. (In Chinese)

64. Li, S.; Shi, S.; Li, L.; Chen, J.; Xu, Z.; Zhou, Z.; Yuan, S. Control of water inrush in typical karst tunnels in three gorges reservoir area and its application. *Chin. J. Rock Mech. Eng.* **2014**, *33*, 1887–1896. (In Chinese)

65. Song, H. *Water Inrush Mechanism of Subsea Tunnel Constructed by Drill-Blasting Method and Its Application*; Beijing Jiaotong University: Beijing, China, 2015. (In Chinese)

66. CCCC Second Highway Consultants Co. Ltd. *Specifications for Design of Highway Underwater Tunnel*; JTG/T 3371—2022; China Communication Press: Beijing, China, 2022. (In Chinese)

67. Zhang, D.; Sun, Z.; Song, H.; Fang, H. Water inrush evolutionary mechanisms of subsea tunnels and process control method. *Chin. J. Rock Mech. Eng.* **2020**, *39*, 649–667. (In Chinese)

68. Valkó, P.; Economides, M.J. Propagation of hydraulically induced fractures—A continuum damage mechanics approach. *Int. J. Rock Mech. Min. Sci. Geomech.* **1994**, *31*, 221–229. [CrossRef]

69. Hubbert, M.K.; Willis, D.G. Mechanics of hydraulic fracturing. *Trans. Am. Inst. Min. Metall. Pet. Eng.* **1972**, *18*, 369–390. [CrossRef]

70. Li, L. *Study on Catastrophe Evolution Mechansim of Karst Water Inrush and Its Eengineering Application of High Risk Karst Tunnel*; Shandong University: Jinan, China, 2009. (In Chinese)

71. Noghabai, K. Effect of various types of fibers on bond capacity-experimental, analytical, and numerical investigations. *Fract. Mech.* **1999**, *182*, 109–128.

72. Wolkersdorfer, C.; Bowell, R.; Walder, I.F.; Nilssen, S.; Räisänen, M.L.; Heikkinen, P.; Pulkkinen, K.; Korkka-Niemi, K.; Salonen, V.P.; Destouni, G. Erratum to: Contemporary Reviews of Mine Water Studies in Europe, Part 2. *Mine Water Environ.* **2012**, *31*, 237–238. [CrossRef]

73. Huang, R.; Wang, X.; Chen, L. Hydro-splitting off analysis on underground water in deep-lying tunnels and its effect on water gushing out. *Chin. J. Rock Mech. Eng.* **2000**, *5*, 573–576. (In Chinese)

74. Liu, Z. *Karst Water Burst Mechanism and Prevention Countermeasures in Yuanliangshan Tunnel*; China University of Geosciences: Wuhan, China, 2004. (In Chinese)

75. Nilsen, B. Characteristics of Water Ingress in Norwegian Subsea Tunnels. *Rock Mech. Rock Eng.* **2014**, *47*, 933–945. [CrossRef]

76. Guo, Y.; Kong, Z.; He, J.; Yan, M. Development and Application of the 3D Model Test System for Water and Mud Inrush of Water-Rich Fault Fracture Zone in Deep Tunnels. *Math. Probl. Eng.* **2021**, *2021*, 8549094. [CrossRef]

77. Meng, R.; Hu, S.; Chen, Y.; Zhou, C. Permeability of non-darcian flow in fractured rock mass under high seepage pressure. *Chin. J. Rock Mech. Eng.* **2014**, *33*, 1756–1764. (In Chinese)

78. Jin, D.; Ng, Y.C.H.; Han, B.; Yuan, D. Modeling Hydraulic Fracturing and Blow-Out Failure of Tunnel Face During Shield Tunneling in Soft Soils. *Int. J. Geomech.* **2022**, *22*, 06021041. [CrossRef]

79. Zhang, D. Deformation control techniques of unfavorable geologic bodies and discontinuous surfaces in subsea tunnel. *Chin. J. Rock Mech. Eng.* **2007**, *26*, 2161–2169. (In Chinese)

80. Tsuji, H.; Sawada, T.; Takizawa, M. Extraordinary inundation accidents in the Seikan undersea tunnel. *Int. J. Rock Mech. Min. Sci. Geomech. Abstr.* **1996**, *33*, 330A. [CrossRef]

81. Gu, Y.; Li, X.; Zhao, Y.; Ren, S. Analysis of forming reason of mud breakout in Tong-Yu tunnel. *Rock Soil Mech.* **2005**, *26*, 920–923. (In Chinese)

82. Yuan, J.; Chen, W.; Tan, X.; Yang, D.; Wang, S. Countermeasures of water and mud inrush disaster in completely weathered granite tunnels: A case study. *Environ. Earth Sci.* **2019**, *78*, 1–16. [CrossRef]

83. Shi, W.; Qiu, J.; Zhang, C.; Wang, Q.; Lai, J.; Li, B.; Mao, Z. Immersion mode and spatiotemporal distribution characteristic of water migration in loess tunnel. *Arab. J. Geosci.* **2022**, *15*, 1–22. [CrossRef]

84. Qiu, J.; Fan, F.; Zhang, C.; Lai, J.; Wang, K.; Niu, F. Response Mechanism of Metro Tunnel Structure under Local Collapse in Loess Strata. *Environ. Earth Sci.* **2022**, *81*, 1–18. [CrossRef]

85. Li, L.; Wang, Q.; Li, S.; Huang, H.; Shi, S.; Wang, K.; Lei, T.; Chen, D. Cause Analysis of Soft and Hard Rock Tunnel Collapse and Information Management. *Pol. J. Environ. Stud.* **2014**, *23*, 1227–1233.

86. Zhang, N.; Shen, J.S.; Zhou, A.; Arulrajah, A. Tunneling induced geohazards in mylonitic rock faults with rich groundwater: A case study in Guangzhou. *Tunn. Undergr. Space Technol.* **2018**, *74*, 262–272. [CrossRef]

87. Nilsen, B. Cases of instability caused by weakness zones in Norwegian tunnels. *Bull. Eng. Geol. Environ.* **2011**, *70*, 7–13. [CrossRef]

88. Pan, D.; Li, S.; Xu, Z.; Lin, P.; Huang, X. Experimental and numerical study of the water inrush mechanisms of underground tunnels due to the proximity of a water-filled karst cavern. *Bull. Eng. Geol. Environ.* **2019**, *78*, 6207–6219. [CrossRef]

89. Fang, Q.; Song, H.; Zhang, D. Complex variable analysis for stress distribution of an underwater tunnel in an elastic half plane. *Int. J. Numer. Anal. Methods Geomech.* **2015**, *39*, 1821–1835. [CrossRef]

90. Chen, J.; Wu, L.; Yan, T. *Dixia Jianzhu Jiegou*; China Communications Press: Beijing, China, 2008.

91. Wang, J.; Feng, B.; Zhang, X.; Tang, Y.; Yang, P. Hydraulic failure mechanism of karst tunnel surrounding rock. *Chin. J. Rock Mech. Eng.* **2010**, *29*, 1363–1370. (In Chinese)

92. Lee, H.S.; Son, B.K.; Lim, Y.G.; Jeon, S.W. Discrete fracture network and equivalent hydraulic conductivity for tunnel seepage analysis in rock mass. *Tunn. Undergr. Space Technol.* **2006**, *21*, 403. [CrossRef]

93. Li, L.; Li, S.; Zhang, Q. Study of mechanism of water inrush induced by hydraulic fracturing in karst tunnels. *Rock Soil Mech.* **2010**, *31*, 523–528. (In Chinese)

94. Zhang, C.; Shu, L.; Appiah-Adjei, E.K.; Lobeyo, A.G.A.; Tang, R.; Fan, J. Laboratory simulation of groundwater hydraulic head in a karst aquifer system with conduit and fracture domains. *Carbonates Evaporites* **2016**, *31*, 329–337. [CrossRef]

95. Zhou, M.; Fang, Q.; Peng, C. A mortar segment-to-segment contact method for stabilized total-Lagrangian smoothed particle hydrodynamics. *Appl. Math. Model.* **2022**, *107*, 20–38. [CrossRef]

96. Li, W.; Zhang, C.; Zhang, D.; Ye, Z.; Tan, Z. Face stability of shield tunnels considering a kinematically admissible velocity field of soil arching. *J. Rock Mech. Geotech. Eng.* **2022**, *14*, 505–526. [CrossRef]

97. Xue, Y.; Wang, D.; Li, S.; Qiu, D.; Li, Z.; Zhu, J. A risk prediction method for water or mud inrush from water-bearing faults in subsea tunnel based on cusp catastrophe model. *KSCE J. Civ. Eng.* **2017**, *21*, 2607–2614. [CrossRef]

98. Li, P.; Wang, F.; Long, Y.; Zhao, X. Investigation of steady water inflow into a subsea grouted tunnel. *Tunn. Undergr. Space Technol.* **2018**, *80*, 92–102. [CrossRef]

99. Li, R.; Zhang, D.; Wu, P.; Fang, Q.; Li, A.; Cao, L. Combined Application of Pipe Roof Pre-SUPPORT and Curtain Grouting Pre-Reinforcement in Closely Spaced Large Span Triple Tunnels. *Appl. Sci.* **2020**, *10*, 3186. [CrossRef]

100. Strømsvik, H. The significance of hydraulic jacking for grout consumption during high pressure pre-grouting in Norwegian tunnelling. *Tunn. Undergr. Space Technol.* **2019**, *90*, 357–368. [CrossRef]

101. Zhang, L.; Yu, R.; Zhang, Q.; Liu, R.; Feng, H.; Chu, Y. Permeation grouting diffusion mechanism of quick setting grout. *Tunn. Undergr. Space Technol.* **2022**, *124*, 104449. [CrossRef]

102. Zhang, M.; Zhang, W.; Sun, G. Evaluation technique of grouting effect and its application to engineering. *Chin. J. Rock Mech. Eng.* **2006**, *25*, 3909–3918. (In Chinese)

103. Wang, Y.; Sun, P.; Han, Z. Pre-grouting and after-grouting for rock tunnelling engineering. *Water Resour. Hydropower Eng.* **2006**, *37*, 31–34. [CrossRef]

104. Wang, Y.; Ma, D.; Ling, S.; Chen, Y. Grouting technology of tunnelling construction in submarine developing belt of permeable channel. *Rock Soil Mech.* **2011**, *32*, 3660–3666. (In Chinese)

105. Bezuijen, A.; Te Grotenhuis, R.; Van Tol, A.F.; Bosch, J.W.; Haasnoot, J.K. Analytical model for fracture grouting in sand. *J. Geotech. Geoenviron. Eng.* **2011**, *6*, 611–620. [CrossRef]

106. Eklund, D.; Stille, H. Penetrability due to filtration tendency of cement-based grouts. *Tunn. Undergr. Space Technol.* **2008**, *23*, 389–398. [CrossRef]

107. Takata, T.; Seki, H.; Matsumoto, T.; Fujii, M.; Oknao, T.; Imai, K. Field tests on improvement effects of fracture grouting in residential areas. *AIJ J. Technol. Des.* **2010**, *16*, 483–488. [CrossRef]

108. Zhang, D.; Sun, Z.; Chen, T. Composite grouting technology for subsea tunnels and its engineering application. *Chin. J. Rock Mech. Eng.* **2019**, *38*, 1102–1116. (In Chinese)

109. Sun, F. *Study on the Key Technique of Composite Grouting for Water Blockage in Weathered Slot of Subsea Tunnel*; Beijing Jiaotong University: Beijing, China, 2010. (In Chinese)

110. Yang, G.; Wang, X.; Wang, X.; Cao, Y. Analyses of seepage problems in a subsea tunnel considering effects of grouting and lining structure. *Mar. Geores. Geotechnol.* **2016**, *34*, 65–70. [CrossRef]

111. Kim, D.R.; Kim, H.J.; Shin, J.H. Performance evaluation of pin-holed pipe anchor for fractured zone in subsea tunnel. *Mar. Geores. Geotechnol.* **2017**, *35*, 769–779. [CrossRef]

112. Jin, W.; Zhang, Y. Fire's effect on chloride ingress related durability of concrete structure. *J. Zhejiang Univ. Sci. A* **2007**, *8*, 675–681. [CrossRef]

113. Figala, P.; Drochytka, R.; Cerny, V.; Hermann, R.; Kolisko, J. Monitoring of Chemical Resistance of New Grouting Materials. *Key Eng. Mater.* **2021**, *6186*, 27–33. [CrossRef]

114. Lu, H.; Zhu, C.; Liu, Q. Study on shear mechanical properties of structural planes grouted with different materials. *Chin. J. Rock Mech. Eng.* **2021**, *40*, 1803–1811. (In Chinese)

115. Li, S.; Ma, C.; Liu, R.; Chen, M.; Yan, J.; Wang, Z.; Duan, S.; Zhang, H. Super-absorbent swellable polymer as grouting material for treatment of karst water inrush. *Int. J. Min. Sci. Technol.* **2021**, *31*, 753–763. [CrossRef]

116. Li, Z.; You, H.; Gao, Y.; Wang, C.; Zhang, J. Effect of ultrafine red mud on the workability and microstructure of blast furnace slag-red mud based geopolymeric grouts. *Powder Technol.* **2021**, *392*, 610–618. [CrossRef]

117. Han, Y.; Xia, J.; Yu, L.; Su, Q.; Chen, M. The relationship between compressive strength and pore structure of the high water Grouting Material. *Crystals* **2021**, *11*, 865. [CrossRef]

118. Wang, H.; Tong, M. Properties and field application of the grouting material for water blocking during thawing of frozen wall of deep sand layer. *Arab. J. Geosci.* **2021**, *14*, 1–12. [CrossRef]

119. Song, J.; Liu, B.; Chu, Z.; Ren, D.; Song, Y. Type Classification and Main Characteristics of Tunnel Collapses. *China Railw. Sci.* **2018**, *39*, 44–51. [CrossRef]

120. Wu, K.; Shao, Z.; Qin, S.; Wei, W.; Chu, Z. A critical review on the performance of yielding supports in squeezing tunnels. *Tunn. Undergr. Space Technol.* **2021**, *115*, 103815. [CrossRef]

121. Liu, C.; Zhou, S.; Yu, C.; Ma, E.; Kong, F.; Tang, X.; Gao, X.; Zhang, X.; Lai, J. Damage behaviours of new-to-old concrete interfaces and a damage prediction model of reinforced concrete. *Eur. J. Environ. Civ. Eng.* **2022**, 1981459. [CrossRef]

122. Fu, Y.; Wang, X.; Wang, L.; Li, Y. Foam concrete: A state-of-the-art and state-of-the-practice review. *Adv. Mater. Sci. Eng.* **2020**, *6153602*. [CrossRef]

123. Son, Y.; Ko, T.Y.; Lee, D.; Won, J.; Lee, I.M.; Choi, H. Applicability of liquid air as novel cryogenic refrigerant for subsea tunnelling construction. *Geomech. Eng.* **2021**, *27*, 179–187. [CrossRef]

124. Cheng, X.; Kang, T.; Yue, C.; Du, X. Shock reduction techniques for a submarine tunnel. *Geomech. Eng.* **2019**, *37*, 3781–3804. [CrossRef]

125. Wu, K.; Shao, Z.; Qin, S. A solution for squeezing deformation control in tunnels using foamed concrete: A review. *Constr. Build. Mater.* **2020**, *257*, 119539. [CrossRef]

126. Wu, G.; Chen, W.; Tan, X.; Zhao, W.; Jia, S.; Tian, H. Performance of New Type of Foamed Concrete in Supporting Tunnel in Squeezing Rock. *Int. J. Geomech.* **2020**, *20*, 04019173. [CrossRef]

127. Moritz, B. Yielding elements–requirements, overview and comparison/Stauchelemente–Anforderungen, berblick und Vergleich. *Geomech. Tunn.* **2011**, *4*, 221–236. [CrossRef]

128. Tan, X.; Chen, W.; Liu, H.; Chan, A.H.C.; Tian, H.; Meng, X.; Wang, F.; Deng, X. A combined supporting system based on foamed concrete and U-shaped steel for underground coal mine roadways undergoing large deformations. *Tunn. Undergr. Space Technol.* **2017**, *68*, 196–210. [CrossRef]

129. Hu, J.; Liu, W.; Pan, Y.; Zeng, H. Site measurement and study of vertical freezing wall temperatures of a large-diameter shield tunnel. *Adv. Civ. Eng.* **2019**, *2019*, 8231458. [CrossRef]

130. Alzoubi, M.A.; Xu, M.; Hassani, F.P.; Poncet, S.; Sasmito, A.P. Artificial ground freezing: A review of thermal and hydraulic aspects. *Tunn. Undergr. Space Technol.* **2020**, *104*, 103534. [CrossRef]

131. Qin, Y.; Lai, J.; Yang, T.; Zan, W.; Feng, Z.; Liu, T. Failure analysis and countermeasures of a tunnel constructed in loose granular stratumby shallow tunnelling method. *Eng. Fail. Anal.* **2022**, *137*, 106223. [CrossRef]

132. Lee, D.; Choi, H.J.; Pham, K.; Lee, I.M.; Choi, H. Numerical Simulation of Artificial-Freezing Propagation for Subsea-Tunnel Construction: Effect of Refrigerant Temperature and Ground Water. In Proceedings of the 8th International Symposium on Geotechnical Aspects of Underground Construction in Soft Ground, TC204 ISSMGE-IS-SEOUL 2014, Seoul, Korea, 25–27 August 2014; Taylor and Francis-Balkema: Leiden, The Netherlands; pp. 153–157.

133. Berggren, A.L. The Oslofjord Subsea Tunnel, a Case Record. In *Ground Freezing 2000-Frost Action in Soils*; CRC Press: Boca Raton, FL, USA, 2020; pp. 267–272.

134. Hu, X.; Deng, S.; Ren, H. In Situ Test Study on Freezing Scheme of Freeze-Sealing Pipe Roof Applied to the Gongbei Tunnel in the Hong Kong-Zhuhai-Macau Bridge. *Appl. Sci.* **2016**, *7*, 27. [CrossRef]

135. Li, J.; Tang, Y.; Yang, P.; Liu, Q. Dynamic properties of freezing–thawing muddy clay surrounding subway tunnel in Shanghai. *Environ. Earth Sci.* **2015**, *74*, 5341–5349. [CrossRef]

136. Hu, X.; Zhang, L. Artificial Ground Freezing for Rehabilitation of Tunneling Shield in Subsea Environment. In *Advanced Materials Research*; Trans Tech Publications Ltd.: Bäch, Switzerland, 2013; Volume 734, pp. 517–521. [CrossRef]

137. Eiksund, G.R.; Berggren, A.L.; Svano, G. Stabilisation of a Glacifluvial Zone in the Oslofjord Subsea Tunnel with Ground Freezing. In Proceedings of the International Conference on Soil Mechanics and Geotechnical Engineering, Istanbul, Turkey, 27–31 August 2001; pp. 1731–1736.

138. Chen, R.; Cheng, G.; Li, S.; Guo, X.; Zhu, L. Development and prospect of research on application of artificial ground freezing. *Chin. J. Geotech. Eng.* **2000**, *1*, 43–47. (In Chinese)

139. Zhou, X.; Su, L.; He, C.; Guan, J. Horizontal ground freezing method applied to tunneling of Beijing Underground Railway System. *Chin. J. Geotech. Eng.* **1999**, *3*, 63–66. (In Chinese)

140. Wang, M. Current developments and technical issues of underwater traffic tunnel-dicussion on construction scheme of Taiwan strait undersea railway tunnel. *Chin. J Rock Mech. Eng.* **2008**, *11*, 2161–2172. (In Chinese)

141. Wang, L.; Sun, L.; Wang, Z.; Zhang, J. Field monitoring of a subsea shield tunnel during standpipe lifting. *Tunn. Undergr. Space Technol.* **2015**, *45*, 52–62. [CrossRef]

142. Liu, T.; Huang, H.; Yan, Z.; Yan, Z.; Tang, X.; Liu, H. A case study on key techniques for long-distance sea-crossing shield tunneling. *Mar. Geores. Geotechnol.* **2020**, *38*, 786–803. [CrossRef]

143. Kang, S.J.; Kim, J.T.; Cho, G.C. Preliminary study on the ground behavior at shore connection of submerged floating tunnel using numerical analysis. *Geomech. Eng.* **2020**, *21*, 133–142. [CrossRef]

144. Yue, X.; Xie, Y.; Xie, Y. The deformation characteristics of weak foundation with high back siltation in the immersed tunnel. *Adv. Mater. Sci. Eng.* **2018**, *2018*, 1–14. [CrossRef]

145. Yang, W.; Tsang, C.K.; Cai, Y.; Hu, Y. Whole-Process risk Management of Subsea Tunnel Engineering. In Proceedings of the Institution of Civil Engineers-Civil Engineering; Thomas Telford Ltd.: London, UK, 2018; Volume 173, pp. 27–34. [CrossRef]

146. Wang, X.; Fan, F.; Lai, J. Strength behavior of circular concrete-filled steel tube stub columns under axial compression: A review. *Constr. Build. Mater.* **2022**, *322*, 126144. [CrossRef]

147. Egeli, I.; Gurbuz, C. Dynamic analysis of an immersed tunnel in Izmir. *Rev. Constr.* **2018**, *17*, 103–111. [CrossRef]

148. Basnet, C.B.; Panthi, K.K. Analysis of unlined pressure shafts and tunnels of selected Norwegian hydropower projects. *J. Rock Mech. Geotech. Eng.* **2018**, *10*, 486–512. [CrossRef]

149. Mahmoodzadeh, A.; Mohammadi, M.; Noori, K.M.G.; Khishe, M.; Ibrahim, H.H.; Ali, H.F.H.; Abdulhamid, S.N. Presenting the best prediction model of water inflow into drill and blast tunnels among several machine learning techniques. *Autom. Constr.* **2021**, *127*, 103719. [CrossRef]

150. Li, S.; Jin, H.; Hu, S.; Manhica, J.F.; Xie, B.; Liu, H.; Tan, X.; Zhou, F. Experimental investigation and field application of pulse-jet cartridge filter in TBM tunneling construction of Qingdao Metro Line 8 subsea tunnel. *Tunn. Undergr. Space Technol.* **2021**, *108*, 103690. [CrossRef]

151. Xue, Y.; Zhou, B.; Wu, Z.; Gao, H.; Qiu, D.; Li, G.; Fu, K. Mechanical Properties of Support Forms for Fault Fracture Zone in Subsea Tunnel. *Soil Mech. Found. Eng.* **2020**, *56*, 436–444. [CrossRef]

152. Liu, R.; Liu, Y.; Xin, D.; Li, S.; Zheng, Z.; Ma, C.; Zhang, C. Prediction of water inflow in subsea tunnels under blasting vibration. *Water* **2018**, *10*, 1336. [CrossRef]

153. Wang, M.; Lu, J.; Liu, D.; Zhang, J. Study of absolute deformation control criterion and its application for large section subsea tunnel with CRD method. *Rock Soil Mech.* **2010**, *3*, 3354–3360. (In Chinese)

154. Zheng, Y.; Wu, K.; Jiang, Y.; Chen, R.; Duan, J. Optimization and design of pre-reinforcement for a subsea tunnel crossing a fault fracture zone. *Mar. Geores. Geotechnol.* **2021**, *3*, 1–18. [CrossRef]

155. Liu, X.; Ma, E.; Liu, J.; Zhang, B.; Niu, D.; Wang, Y. Deterioration of an industrial reinforced concrete structure exposed to high temperatures and dry-wet cycles. *Eng. Fail. Anal.* **2022**, *135*, 106150. [CrossRef]

156. Li, S.; Tian, H.; Xue, Y.; Su, M.; Qiu, D.; Li, P.; Li, Z. Study on major construction disasters and controlling technology at the Qingdao Kiaochow Bay subsea tunnel. *J. Coast. Res.* **2015**, *73*, 403–409. [CrossRef]

157. Huang, C.; Zhang, S.; Wu, S.; Gao, Y. Research and application of a comprehensive forecasting system for tunnels in water-bearing fault fracture zones: A case study. *Arab. J. Geosci.* **2022**, *15*, 1–16. [CrossRef]

158. Kim, Y.; Lee, S.S. A Study of the Effects of Geological Conditions on Korean Tunnel Construction Time Using the Updated NTNU Drill and Blast Prediction Model. *Appl. Sci.* **2021**, *11*, 10096. [CrossRef]

159. Li, S.; Liu, B.; Xu, X.; Nie, L.; Liu, Z.; Song, J.; Sun, H.; Chen, L.; Fan, K. An overview of ahead geological prospecting in tunneling. *Tunn. Undergr. Space Technol.* **2017**, *63*, 69–94. [CrossRef]

160. Wang, S.; Li, S.; Li, L.; Shi, S.; Zhou, Z.; Cheng, S.; Hu, H. Study on early warning method for water inrush in tunnel based on fine risk evaluation and hierarchical advance forecast. *Geosciences* **2019**, *9*, 392. [CrossRef]

161. Xue, Y.; Li, Z.; Li, S.; Qiu, D.; Su, M.; Xu, Z.; Zhou, B.; Tao, Y. Water inrush risk assessment for an undersea tunnel crossing a fault: An analytical model. *Mar. Geores. Geotechnol.* **2019**, *37*, 816–827. [CrossRef]

162. Zhang, L.; Zhao, D.; Wu, J.; Yang, W.; Wang, W.; Xin, D. Prediction of water inflow in Tsingtao subsea tunnel based on the superposition principle. *Tunn. Undergr. Space Technol.* **2020**, *97*, 103243. [CrossRef]

163. Li, S.; Song, J.; Zhang, J.; Wang, C.; Liu, B.; Liu, F.; Ma, S.; Nie, L. A New Comprehensive Geological Prediction Method Based on Constrained Inversion and Integrated Interpretation for Water-Bearing Tunnel Structures. *Eur. J. Environ. Civ. Eng.* **2017**, *21*, 1441–1465. [CrossRef]

164. Li, S.; Sun, H.; Li, X.; Lu, X.; Xue, Y.; Su, M. Advanced geology prediction with parallel transient electromagnetic detection in tunnelling. *Chin. J. Rock Mech. Eng.* **2014**, *33*, 1309–1318. (In Chinese)

165. Xue, Y.; Li, S.; Su, M.; Li, S.; Zhang, Q.; Zhao, Y.; Li, W. Study of geological prediction implementation method in tunnel construction. *Rock Soil Mech.* **2011**, *32*, 2416–2422. (In Chinese)

166. Liu, B.; Nie, L.; Li, S.; Xu, L.; Liu, Z.; Song, J.; Li, L.; Lin, C. 3D Electrical resistivity inversion tomography with spatial structural constraint. *Chin. J. Rock Mech. Eng.* **2012**, *31*, 2258–2268. (In Chinese)

167. Li, D.; Liu, Y.; Wang, M.; Zhang, D. Controlling Technology Research of Deforming due to South-to-North Water Transfer Tunnel Down Crossing Subway. In *Advanced Materials Research*; Thomas Telford Ltd.: London, UK, 2012; Volume 594, pp. 1290–1293. [CrossRef]

168. Xu, T.; Zhang, D.; Li, A.; Fang, Q.; Yu, L.; Li, R. Dissecting the Robustness of the Rock Mass Classification Methods Used in Jiaozhou Bay Subsea Tunnel. *Int. J. Civ. Eng.* **2021**, *19*, 1473–1482. [CrossRef]

169. Cao, L.; Zhang, D.; Fang, Q. Semi-analytical prediction for tunnelling-induced ground movements in multi-layered clayey soils. *Tunn. Undergr. Space Technol.* **2020**, *102*, 103446. [CrossRef]

170. Hu, W. *Theory and Method of Mine Water Harzard Prevention and Control*; China Coal Industry Publishing House: Chaoyang, China, 2005.

171. Chen, F.; Ma, T.; Tang, C.; Du, Y.; Li, Z.; Liu, F. Research on the law of large-scale deformation and failure of soft rock based on microseismic monitoring. *Adv. Civ. Eng.* **2018**, *2018*, 1–8. [CrossRef]

172. Tang, S.; Tong, M.; Hu, J. Study on Prediction of Water Inrush in Mine by Microseismic Technique. In Proceedings of the 2009 International Workshop on Intelligent Systems and Applications, IEEE, Wuhan, China, 23–24 May 2009; pp. 1–4. [CrossRef]

173. Tang, C.; Li, L.; Xu, N.; Ma, K. Microseismic monitoring and numerical simulation on the stability of high-steep rock slopes in hydropower engineering. *J. Rock Mech. Geotech. Eng.* **2015**, *7*, 493–508. (In Chinese) [CrossRef]

174. Qian, Q. Challenges faced by underground projects construction safety and countermeasures. *Chin. J. Rock Mech. Eng.* **2012**, *31*, 1945–1956. (In Chinese)

175. Li, G.; Zhu, F.; Ren, L.; Tian, X.; Zhao, N. Application of microseismic technology in monitoring waterflood front in Gaoshangpu mid-deep reservoirs. *Spec. Oil Gas Reserv.* **2010**, *17*, 104–106.

176. Li, T.; Mei, T.; Sun, X.; Lv, Y.; Sheng, J.; Cai, M. study on a water-inrush incident at Laohutai coalmine. *Int. J. Rock Mech. Min. Sci.* **2013**, *59*, 151–159. [CrossRef]

177. Chen, D. *Study on Water Inrush Mechanism and Real-Time Monitoring Method of Karst Cave in Tunnels*; Shandong University: Jinan, China, 2016.

178. Li, H.; Jia, F.; Li, J.; Li, S. Key technologies for design of subsea tunnel of Dalian metro line 5. *Rock Soil Mech.* **2017**, *38*, 395–401. (In Chinese)

179. Zhang, Y.; Fan, S.; Yang, D.; Zhou, F. Investigation About Variation Law of Frost Heave Force of Seasonal Cold Region Tunnels: A Case Study. *Front. Earth Sci.* **2022**, *9*, 806843. [CrossRef]

180. Deng, Y. Hydrogeological change characteristics and treatment measures caused by long-term drainage in deep karst water section of Dayaoshan tunnel. *Hydrogeol. Eng. Geol.* **1992**, *6*, 44–49. (In Chinese)

181. Zhang, C.; Zhang, D.; Wang, M.; Guo, X. Study and engineering application of waterproofing and drainage system in Xiamen subsea tunnel. *China J. Highw. Transp.* **2008**, *3*, 69–75. (In Chinese)

182. Wang, Y.; Wang, X.; Chen, J. Research on Effect of Grouting Circle on Seepage Field of Subsea Tunnel. In *Applied Mechanics and Materials*; Thomas Telford Ltd.: London, UK, 2012; Volume 204, pp. 1409–1412. [CrossRef]

183. Zhang, D.; Sun, Z. An active control waterproof and drainage system of subsea tunnels and its design method. *Chin. J. Rock Mech. Eng.* **2019**, *38*, 1–17. (In Chinese)

184. Zhang, Y.; Zhang, D.; Fang, Q.; Xiong, L.; Yu, L.; Zhou, M. Analytical solutions of non-Darcy seepage of grouted subsea tunnels. *Tunn. Undergr. Space Technol.* **2020**, *96*, 103182. [CrossRef]